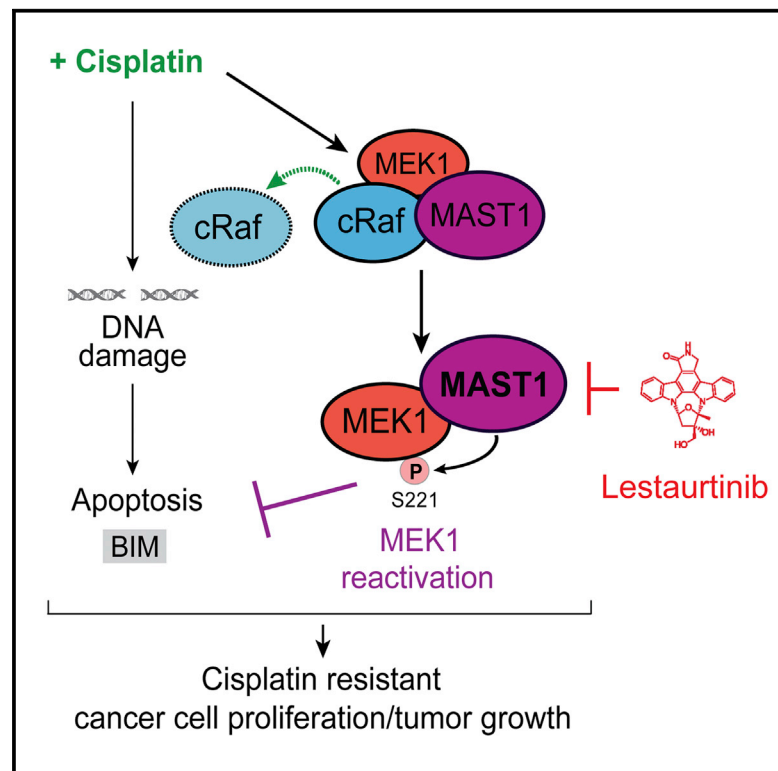


Cancer Cell

MAST1 Drives Cisplatin Resistance in Human Cancers by Rewiring cRaf-Independent MEK Activation

Graphical Abstract



Authors

Lingtao Jin, Jaemoo Chun, Chaoyun Pan, ..., Dong M. Shin, Sagar Lonial, Sumin Kang

Correspondence

smkang@emory.edu

In Brief

Jin et al. show that cisplatin dissociates cRaf from MEK1 to inhibit the MAPK pathway and identify MAST1 as a main cisplatin resistance driver that replaces cRaf to reactivate the MAPK pathway. They further show that inhibition of MAST1 by the multi-kinase inhibitor lestaurtinib restores cisplatin sensitivity.

Highlights

- MAST1 is a synthetic lethal target for cisplatin therapy in cancer cells
- Cisplatin binds to MEK1 and dissociates cRaf but not MAST1 from MEK1
- MAST1 replaces cRaf to reactivate the MAPK pathway and confer cisplatin resistance
- Lestaurtinib is a promising MAST1 inhibitor

MAST1 Drives Cisplatin Resistance in Human Cancers by Rewiring cRaf-Independent MEK Activation

Lingtao Jin,¹ Jaemoo Chun,¹ Chaoyun Pan,¹ Dan Li,¹ Ruiting Lin,¹ Gina N. Alesi,¹ Xu Wang,¹ Hee-Bum Kang,¹ Lina Song,² Dongsheng Wang,¹ Guojing Zhang,¹ Jun Fan,³ Titus J. Boggon,⁴ Lu Zhou,⁵ Jeanne Kowalski,⁶ Cheng-Kui Qu,^{1,7} Conor E. Steuer,¹ Georgia Z. Chen,¹ Nabil F. Saba,¹ Lawrence H. Boise,¹ Taofeek K. Owonikoko,¹ Fadlo R. Khuri,¹ Kelly R. Magliocca,⁸ Dong M. Shin,¹ Sagar Lonial,¹ and Sumin Kang^{1,9,*}

¹Department of Hematology and Medical Oncology, Winship Cancer Institute of Emory, Emory University School of Medicine, Atlanta, GA 30322, USA

²Department of Neuroscience, Morehouse School of Medicine, Atlanta, GA 30310, USA

³Department of Radiation Oncology, Emory University School of Medicine, Atlanta, GA 30322, USA

⁴Department of Pharmacology, Yale University School of Medicine, New Haven, CT 06520, USA

⁵School of Pharmacy, Fudan University, Shanghai 201203, China

⁶Department of Biostatistics and Bioinformatics, Emory University School of Public Health, Atlanta, GA, USA

⁷Department of Pediatrics, Emory University School of Medicine, Atlanta, GA 30322, USA

⁸Department of Pathology & Laboratory Medicine, Emory University School of Medicine, Atlanta, GA 30322, USA

⁹Lead Contact

*Correspondence: smkang@emory.edu

<https://doi.org/10.1016/j.ccell.2018.06.012>

SUMMARY

Platinum-based chemotherapeutics represent a mainstay of cancer therapy, but resistance limits their curative potential. Through a kinome RNAi screen, we identified microtubule-associated serine/threonine kinase 1 (MAST1) as a main driver of cisplatin resistance in human cancers. Mechanistically, cisplatin but no other DNA-damaging agents inhibit the MAPK pathway by dissociating cRaf from MEK1, while MAST1 replaces cRaf to reactivate the MAPK pathway in a cRaf-independent manner. We show clinical evidence that expression of MAST1, both initial and cisplatin-induced, contributes to platinum resistance and worse clinical outcome. Targeting MAST1 with lestaurtinib, a recently identified MAST1 inhibitor, restores cisplatin sensitivity, leading to the synergistic attenuation of cancer cell proliferation and tumor growth in human cancer cells and patient-derived xenograft models.

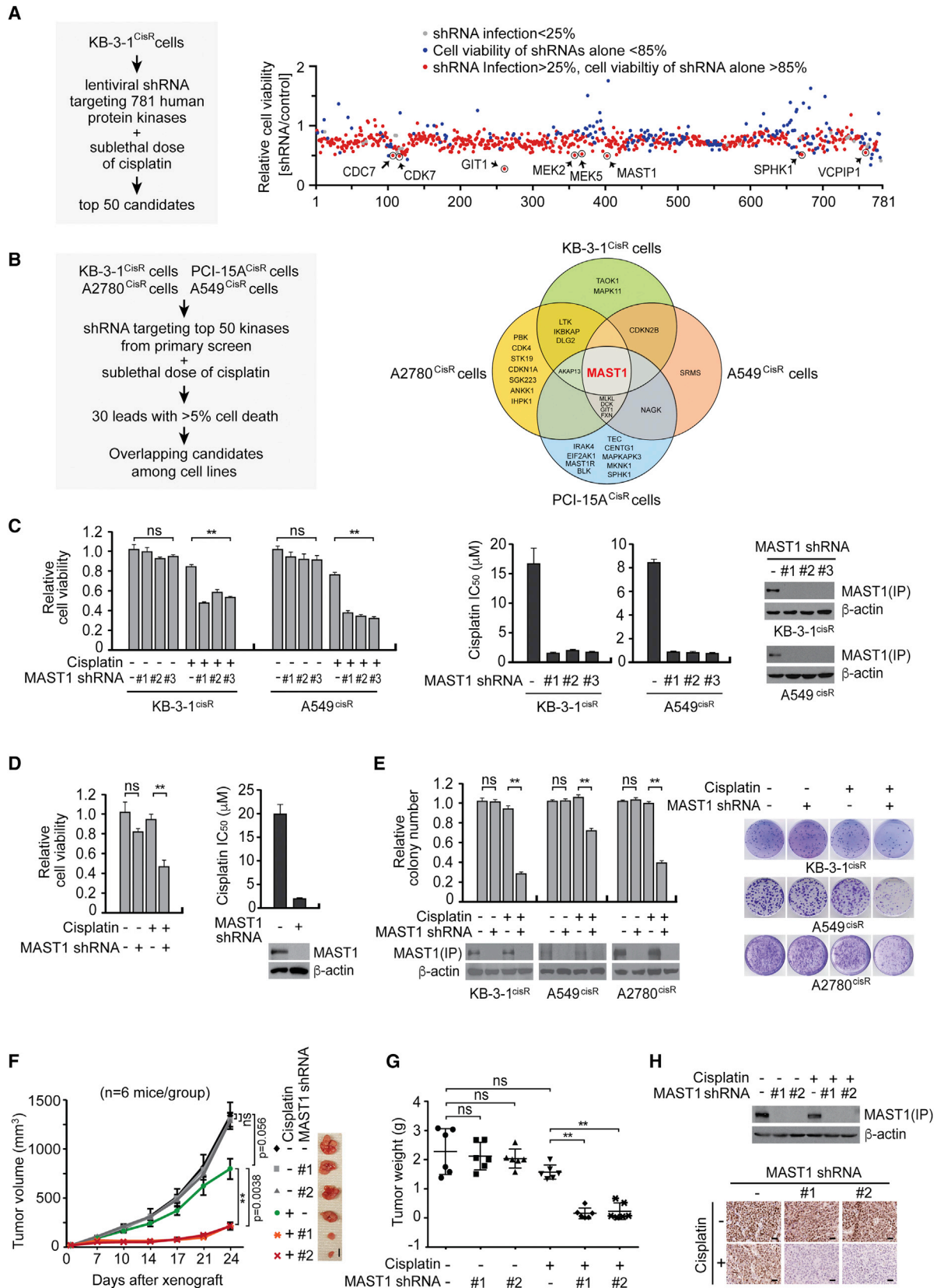
INTRODUCTION

Platinum-based chemotherapy is employed for the treatment of a wide array of solid malignancies including head and neck, lung, and ovarian cancers (Galanski, 2006). Cisplatin and other similar platinum-based drugs lead to an initial therapeutic success, but many patients have tumors that are intrinsically resistant or develop resistance to cisplatin treatment (Giaccone, 2000; Koberle et al., 2010). Cisplatin exerts anti-cancer effects mainly by in-

teracting with DNA to form mostly intrastrand crosslink adducts, which activate pro-apoptotic signal transduction pathways (Siddik, 2003). Cisplatin resistance likely occurs due to complex reasons, including increased drug efflux, drug breakdown, increased repair of damaged DNA, and increased activation of pro-survival pathways or inhibition of pathways that promote cell death (Siddik, 2003). Although a group of signaling effectors have been identified as predictive markers of cisplatin resistance including MRP2 (Liedert et al., 2003), ERCC1 (Metzger et al., 1998), ATPase7A/7B/11B

Significance

Activation of proliferative signaling pathways following chemotherapy has been associated with therapeutic resistance. However, relatively little is known of its mechanism. Our findings provide insights into cancer cisplatin resistance by characterizing the role of MAST1 in driving cisplatin resistance and its mode of action in human cancers involving rewiring of the MEK signaling pathway. We offer a clinical strategy to enhance the susceptibility of cancers to cisplatin by identifying the small-molecule kinase inhibitor lestaurtinib as a potent MAST1 inhibitor and cisplatin-sensitizing agent. These findings not only highlight mechanisms by which MAST1 contributes to the development of cisplatin resistance via the MAPK pathway but also implicate MAST1 as a promising therapeutic target to battle cisplatin-resistant cancers.



(legend on next page)

(Aida et al., 2005; Moreno-Smith et al., 2013), ERBB2 (Fijolek et al., 2006), Bcl-2 (Han et al., 2003), and survivin (Ikeguchi and Kaibara, 2001), most of these studies lacked either an assessment of clinical correlation or an explanation for how these protein factors regulate pro-survival signals in the presence of cisplatin. Therefore, the detailed molecular mechanisms of platinum-based drug resistance still remain elusive.

Protein kinases are often involved in pro-survival signaling pathways (Datta et al., 1997; Persons et al., 2000). The serine/threonine kinase microtubule-associated serine/threonine-protein kinase 1 (MAST1, also known as SAST170) belongs to a family containing four members, MAST1–MAST4. MAST family members share approximately 49%–64% sequence homology and contain four distinct domains including DUF1908, serine/threonine kinase domain, AGC-kinase C-terminal domain, and PDZ domain (Garland et al., 2008). MAST1 is reported to function as a scaffold protein to link the dystrophin/utrophin network with microfilaments via syntrophin (Lumeng et al., 1999). Recurrent rearrangement of the MAST1 gene has been observed in breast cancer cell lines and tissues (Robinson et al., 2011). Nonetheless, little is known about the biological role of MAST1 as a kinase and its role in human cancers.

Higher MEK1 expression in cancers is associated with platinum-based drug resistance and correlates with shortened progression-free survival of patients. Activation of the MAPK family of proteins has been implicated in response to platinum-based chemotherapy. For instance, inhibition of MEK/ERK signaling augmented cisplatin sensitivity in human squamous cell carcinoma (Kong et al., 2015). Although the importance of MEK in cancer and its contribution to chemotherapy response is well studied, the detailed molecular mechanisms by which MEK is activated in response to platinum-based drug treatment, and how it consequently contributes to cisplatin response, is unclear. The goal of this study is to identify and characterize a critical kinase that drives cisplatin resistance in human cancers and evaluate its potential as a chemosensitizing therapeutic target for the treatment of patients with cisplatin-resistant cancer.

RESULTS

MAST1 Is Important for Cisplatin-Resistant Cancer Cell Proliferation and Tumor Growth

To gain insight into the role of protein kinase signaling in cancer chemoresistance, we performed a kinome-wide RNAi screen us-

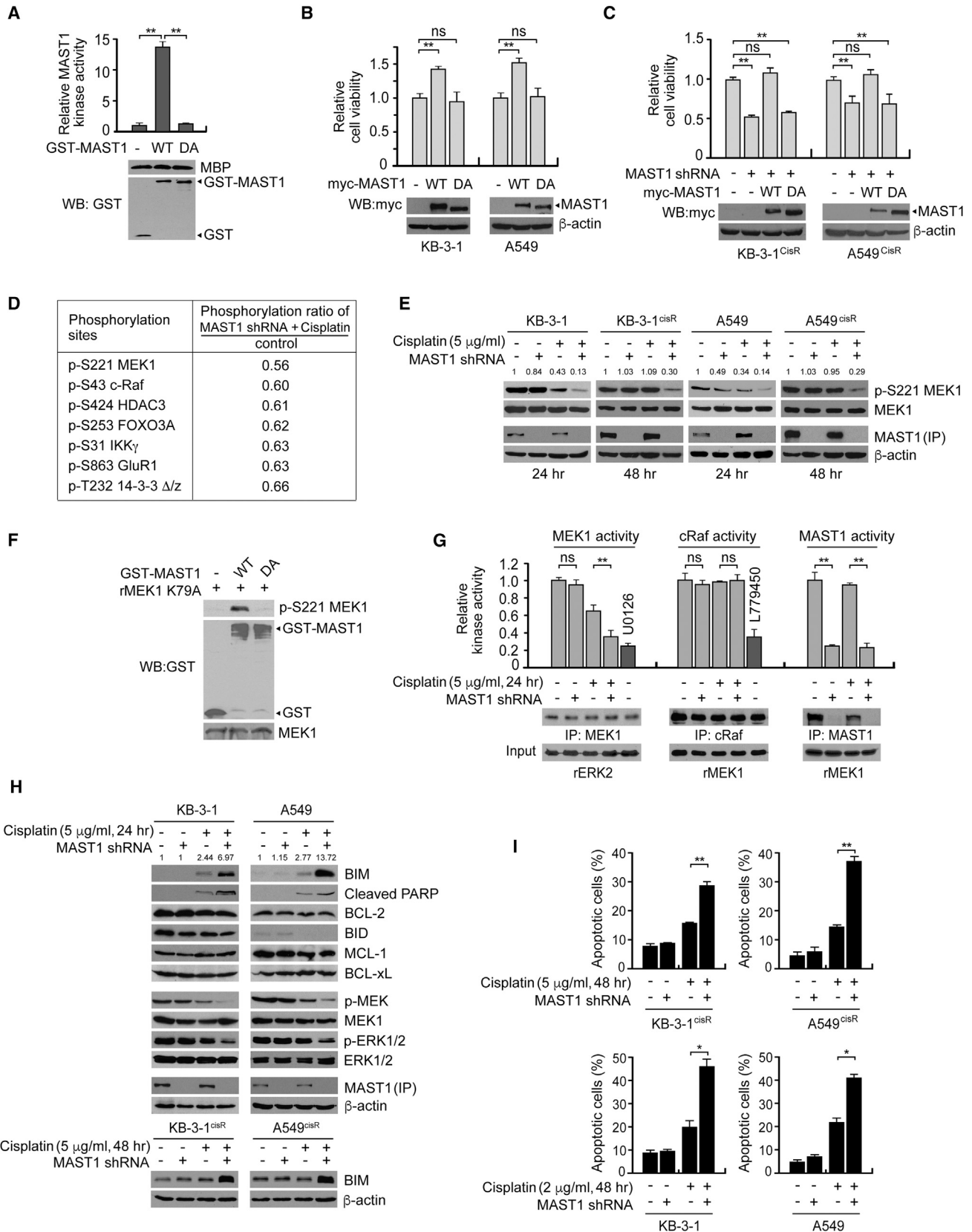
ing a lentiviral short hairpin RNA (shRNA) library targeting 781 human kinase genes and kinase-related genes represented by 4,518 shRNA constructs. The primary screen involved transducing cisplatin-resistant, KB-3-1^{cisR}, or taxol-resistant, KB-3-1^{taxolR}, human carcinoma cell lines and with a lentivirus pool containing shRNAs targeting each of the 781 individual genes, and treating with sublethal doses of cisplatin or taxol (Richert et al., 1985). From the primary screen using KB-3-1^{cisR}, 567 of 781 genes were selected for ranking by excluding shRNAs with low infection efficiency and shRNA clones that alone induced more than 15% cell death (Figure 1A). The secondary screen evaluated the top 50 ranking candidate genes in four cisplatin-resistant cancer cell lines including head and neck squamous cell carcinoma (HNSCC) PCI-15A, lung cancer A549, and ovarian cancer A2780 in addition to KB-3-1 cells (Figures 1B, S1A, and S1B). MAST1 was identified as the third most effective target from the primary screen, and emerged as a lead hit from the secondary screen, as it sensitized cancer cells to cisplatin treatment across cancer types. MAST1 ranked 756 as an effective synthetic lethal target for taxol treatment, suggesting that targeting MAST1 selectively sensitizes cells to the chemotherapy agent cisplatin.

To confirm the screening results for MAST1, we generated MAST1 stable knockdown cells using individual shRNA clones. Targeting MAST1 with three different shRNA clones attenuated cell viability only in the presence of cisplatin in KB-3-1^{cisR} and A549^{cisR} cells (Figure 1C). Moreover, knockdown of MAST1 sensitized TKO-002 cell, which are derived from a patient with platinum-refractory small cell lung carcinoma (SCLC) (Owonikoko et al., 2016), to cisplatin treatment (Figure 1D). Sensitization was observed in cancer cells treated with carboplatin, another platinum-based compound, but not with taxol, demonstrating that the synthetic lethal effect is specific to platinum (Figures S1C and S1D). In addition, MAST1 knockdown attenuated colony-formation potential of cancer cell lines only in the presence of cisplatin (Figure 1E). We next functionally validated this *in vivo*. Xenograft tumors derived from KB-3-1^{cisR} cells with MAST1 knockdown and treated with cisplatin showed a dramatic decrease in tumor growth rate, tumor mass, and tumor proliferation compared with tumors derived from cells with MAST1 knockdown but without cisplatin treatment or to tumors without MAST1 knockdown treated with cisplatin (Figures 1F–1H, S1E, and S1F). These data suggest that MAST1 confers cisplatin resistance and that targeting MAST1 sensitizes cancer cells to cisplatin by acting as a synthetic lethal partner.

Figure 1. Targeting MAST1 Sensitizes Cisplatin Treatment *In Vitro* and *In Vivo*

(A) Primary screen testing 781 genes was carried out using sublethal dose (5 $\mu\text{g}/\text{mL}$) of cisplatin (left). Candidates with low virus infection efficiency (<25%; gray) and shRNAs that alone induced cell death (>15%; blue) were excluded (right).
 (B) Secondary screen used the top 50 candidates from the primary screen in four cisplatin-resistant cancer cell lines (KB-3-1^{cisR}, A549^{cisR}, A2780^{cisR}, and PCI-15A^{cisR}) (left). Thirty leads showing >10% cell death upon shRNA and cisplatin treatment are shown (right).
 (C and D) Cell viability and cisplatin sensitivity of KB-3-1^{cisR} and A549^{cisR} cells (C) and platinum-refractory (cis^R) TKO-002 cells (D) with MAST1 knockdown. Cells were transduced with three different MAST1 shRNA clones followed by sublethal dose of cisplatin (5 $\mu\text{g}/\text{mL}$ for KB-3-1^{cisR} and 2 $\mu\text{g}/\text{mL}$ for A549^{cisR}) or vehicle treatment. Cisplatin IC₅₀ was assessed after 72 hr. IP, immunoprecipitation.
 (E) Colony-formation assays were performed using cancer cells with MAST1 knockdown and cisplatin treatment.
 (F–H) Effect of cisplatin treatment and MAST1 knockdown using two shRNA clones on tumor growth of KB-3-1^{cisR} xenograft mice. Mice were treated with vehicle control or cisplatin 3 days after xenograft and tumor size was monitored (F). Tumor weight (G) and MAST1 expression in tumor lysates (H; top) are shown. Representative images of Ki-67 immunohistochemical (IHC) staining in harvested tumors from each group are shown (H; bottom). Scale bars represent 10 mm (F) and 50 μm (H).

Data are mean \pm SD from three technical replicates of each sample for (C) to (E). Error bars represent SEM (F) and SD (G). p values were determined by two-tailed Student's t test (ns, not significant; **p < 0.01). See also Figure S1.



(legend on next page)

MAST1 Confers Cisplatin Resistance through cRaf-Independent MEK1 Activation

We next explored whether the kinase activity of MAST1 is required to provide cisplatin resistance in cancer cells. Thus, we generated a kinase-dead form of MAST1 by mutating proton acceptor active residue aspartic acid (D) at 497 to alanine (A). D497A mutation in MAST1 abolished its kinase activity (Figure 2A). Overexpression of the wild-type (WT) but not the D497A mutant (DA) MAST1 conferred cisplatin resistance to cisplatin-sensitive parental cells (Figure 2B). Consistently, shRNA-resistant WT but not DA MAST1 rescued the cisplatin resistance attenuated due to MAST1 knockdown in cisplatin-resistant cells (Figure 2C). These data suggest that the kinase activity of MAST1 is required for cancer cells to acquire cisplatin-resistant pro-survival signals.

To investigate the mechanism of MAST1 as a kinase in cisplatin resistance, we performed high-throughput phosphorylation profiling with 1,318 site-specific antibodies from over 30 signaling pathways. We identified a spectrum of proteins whose phosphorylation levels were decreased in KB-3-1^{cisR} cells only when MAST1 was knocked down and cells were treated with cisplatin (Figures 2D and S2A). Among these, a decrease in phosphorylation at S43 of cRaf, which is known to correspond to inhibition of cRaf activity, was observed. However, the greatest decrease was seen in phosphorylation of MEK1 at S221, which is involved in its activation. We next further investigated this by immunoblotting in diverse cell lines. Cisplatin uptake differed between parental and cis^R cells (Figure S2B); therefore, the treatment conditions were adjusted throughout the study so that all cell lines could take up a similar amount of cisplatin. Immunoblotting confirmed that knockdown of MAST1 together with cisplatin treatment in cancer cells did not affect the phosphorylation levels of STAT3 or AKT (Figure S2C) but decreased the phosphorylation levels of MEK1 and its downstream ERK1/2 (Figures 2E and S2D). There was no change or slight increase in Ras and cRaf activity upon MAST1 knockdown and cisplatin treatment, suggesting that the MEK activity decrease is not through its upstream Ras or Raf (Figure S2E). Furthermore, the decreased MEK/ERK activity was rescued by overexpression of WT but not DA MAST1 (Figure S2F). Moreover, MAST1 directly phosphorylates MEK1 at S221 in an *in vitro* MAST1 ki-

nase assay (Figure 2F). Supporting this finding, the kinase activity of MEK1 was significantly decreased, but cRaf activity was not altered, by cisplatin treatment and MAST1 knockdown in KB-3-1 and KB-3-1^{cisR} cells (Figures 2G and S2G). In line with our finding, targeting MEK1 by stable knockdown or its specific inhibitors AZD6244 and trametinib sensitized cancer cells to cisplatin, although MEK1 knockdown itself attenuated cell growth, which was not observed with MAST1 knockdown (Figures S2H and S2I). These results confirmed that MEK1 is a downstream effector of MAST1, which contributes to cisplatin resistance in cancer cells. Moreover, assessment of a group of apoptotic factors revealed that MEK1 and subsequent ERK inactivation upon MAST1 knockdown and cisplatin treatment resulted in the accumulation of pro-apoptotic factor BIM specifically (Figure 2H). Furthermore, MAST1 knockdown together with sublethal doses of cisplatin resulted in enhanced apoptotic cell death (Figure 2I). These data together suggest that MAST1 contributes to cisplatin resistance through a MEK1-mediated anti-apoptotic signaling pathway.

We further explored the molecular mechanism by which MAST1 controls MEK1 activation in the presence of cisplatin. Interestingly, cisplatin does not affect Ras or Raf activity but dissociates cRaf, the known upstream kinase of MEK, from MEK1 in diverse types of cancer cells (Figures 3A and S3A). The dissociation also occurred in cis^R cells, although these cells required more cisplatin to mediate this effect (Figure S3B). Moreover, cisplatin dissociates cRaf from MEK1 in a dose-dependent manner *in vitro* using purified MEK1-cRaf complex isolated from KB-3-1 cells by MEK1 immunoprecipitation, suggesting that cisplatin directly induces dissociation of cRaf from MEK1 (Figure 3B). Biophysical assays including surface plasmon resonance (SPR), thermal shift, and microscale thermophoresis further demonstrated that cisplatin directly binds to MEK1 but not cRaf (Figures 3C and S3C). In addition, co-immunoprecipitation revealed that MAST1 forms a complex with cRaf-MEK1 and cisplatin dissociates cRaf from MEK1, but MAST1 remains within the complex (Figure 3D). In agreement with this, SPR using purified proteins showed that cisplatin binding to MEK1 weakens the interaction of MEK1 with cRaf, but not MAST1 (Figure 3E). SPR-based kinetic analyses of the binding between cisplatin and MEK1 using MEK1 cysteine mutants revealed that the C142

Figure 2. MAST1 Directly Phosphorylates MEK1 and Activates Anti-apoptotic Signaling upon Cisplatin Treatment

(A) MAST1 *in vitro* kinase assay using MAST1 wild-type (WT) or kinase-dead mutant (DA; D497A). GST-MAST1 variants were enriched from 293T and kinase activity was assessed by ADP-Glo Kinase assay using myelin basic protein (MBP) as a substrate.

(B) Cell viability of parental cancer cells with WT or DA MAST1 overexpression in the presence of cisplatin.

(C) Cell viability of cisplatin-resistant (cis^R) cells with endogenous MAST1 knockdown and expression of shRNA-resistant WT or DA MAST1. Relative viability was obtained by normalizing values to cisplatin untreated samples for (B) and (C).

(D) Phospho-antibody array results using 1,318 antibodies in KB-3-1^{cisR} lysates. Top seven protein factors whose phosphorylation states decreased in MAST1 knockdown and cisplatin treatment are shown.

(E) Parental and cis^R pairs of KB-3-1 and A549 cells with MAST1 knockdown and cisplatin treatment (5 μ g/mL) were assayed for MEK1 phosphorylation by immunoblotting.

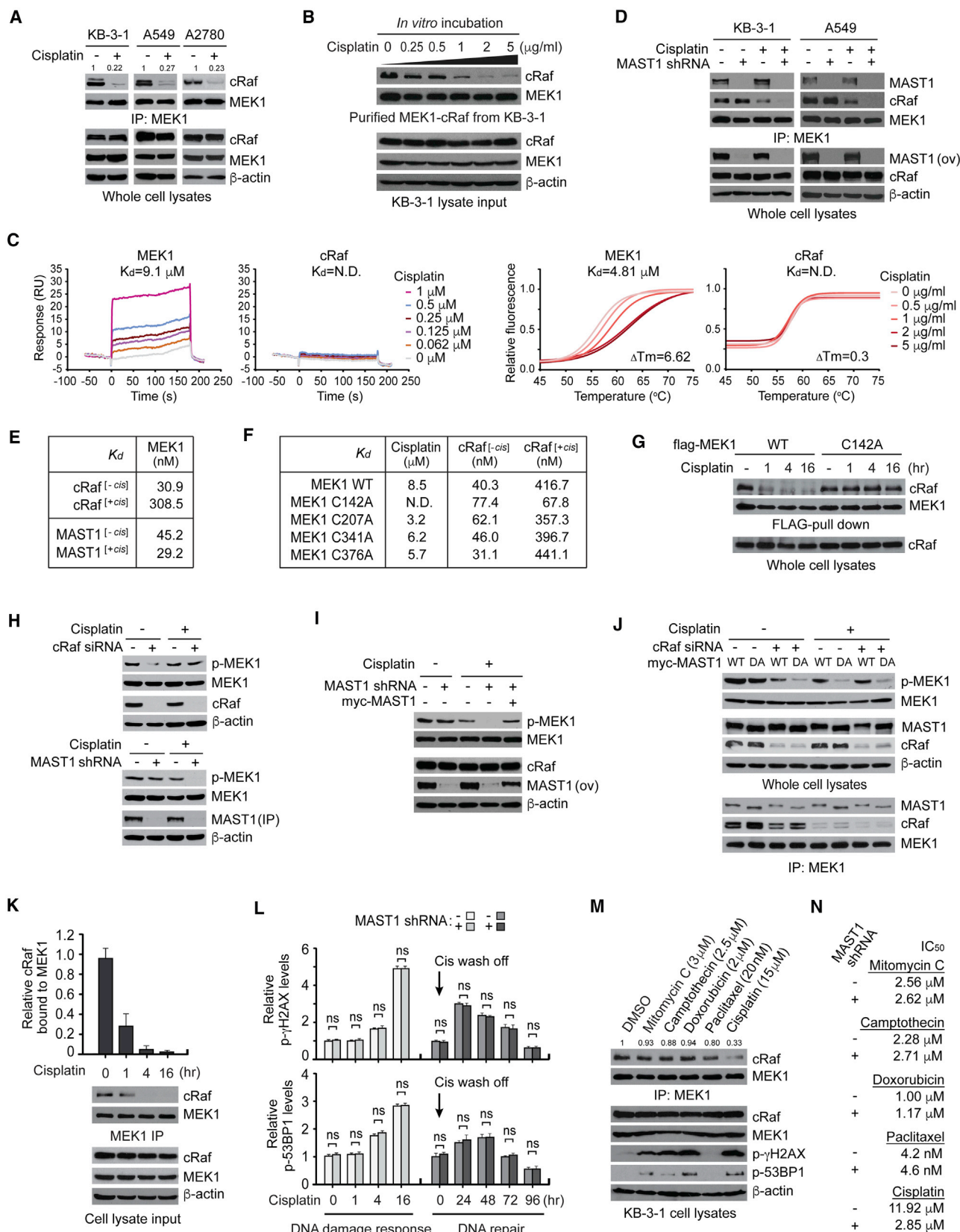
(F) MAST1 *in vitro* kinase assay using recombinant inactive MEK1 (rMEK1 K79A) as a substrate.

(G) Kinase activities of MEK1, cRaf and MAST1 in cells with MAST1 knockdown and cisplatin treatment. MEK1, cRaf and MAST1 were immunoprecipitated from KB-3-1 cells and kinase activities were determined by ADP-Glo kinase assay using recombinant inactive ERK2 or MEK1 as substrates. MEK inhibitor U0126 (10 μ M) and Raf inhibitor L779450 (5 μ M) were used as controls.

(H) Western blot analysis of apoptosis-related factors. Cells with or without MAST1 shRNA were treated with cisplatin (5 μ g/mL) for 24 hr.

(I) Apoptosis assay using parental and cis^R cells with or without MAST1 knockdown. Cells were treated with sublethal dose of cisplatin (2 μ g/mL, parental; 5 μ g/mL, cis^R) for 48 hr and apoptotic cells were assayed by annexin V staining.

Error bars represent \pm SD from three technical replicates. p values were determined by two-tailed Student's t test (ns, not significant; *0.01 < p < 0.05; **p < 0.01). See also Figure S2.



residue is responsible for cisplatin binding (Figures 3F and S3D). Cisplatin binding-deficient mutant MEK1 C142A was unable to separate cRaf from MEK1 in the presence of cisplatin *in vitro* (Figures 3F and S3E). Moreover, the C142A MEK1 neither separated cRaf from MEK1-cRaf complex nor attenuated MEK activity in cells in response to cisplatin, suggesting that cisplatin binds MEK1 and directly promotes the dissociation of cRaf (Figures 3G and S3F). MEK1 knockdown did not influence the MAST1 and cRaf interaction, suggesting that multiple binding sites exist in the complex, and MAST1 is coupled with cRaf not through MEK1 (Figure S3G). Next, we investigated whether cisplatin affects the dependency of MEK1 on MAST1 or cRaf. Knockdown of cRaf decreased MEK1 phosphorylation in the absence but not the presence of cisplatin (Figure 3H). In contrast, MEK1 phosphorylation was decreased by MAST1 knockdown in the presence but not the absence of cisplatin (Figure 3H), and the decreased phosphorylation of MEK1 was restored by rescue expression of MAST1 in MAST1 knockdown cells with cisplatin (Figure 3I). Furthermore, in the presence of cisplatin, MAST1 WT but not MAST1 kinase-dead mutant DA induced MEK1 activation regardless of cRaf knockdown (Figure 3J). MEK1 activation status was also monitored by ERK phosphorylation (Figure S3H). These results suggest that cisplatin switches cRaf-dependent MEK1 activation to MAST1 dependence in cancer cells.

To further explore whether the cisplatin-mediated switch to MAST1 dependence is a result of DNA-damage response signaling, we examined the timing of the switch and the impact of MAST1 on cisplatin-DNA adduct and on DNA damage and repair in time-course analyses. cRaf dissociated from MEK1 upon cisplatin treatment within 1 hr regardless of Raf activation such as Braf V600E. However, cisplatin induced reactive oxygen species and consequently activated Ras, and the MEK/ERK cascade overshadowed the effect of dissociation on

MEK/ERK suppression in the early hours of treatment; this was abolished by treatment with anti-oxidant N-acetyl-cysteine (NAC). Cisplatin-induced DNA damage, by contrast, was a later event, suggesting that MEK/ERK suppression is not a secondary effect of cisplatin treatment but occurs through cRaf-MEK1 dissociation (Figures 3K, S3I, and S3J). In addition, loss of MAST1 had no impact on DNA damage/repair and cisplatin adduct accumulation/removal (Figures 3L, S3K, and S3L). Moreover, MAST1 knockdown did not affect the Fanconi anemia DNA-repair pathway and DNA-damage response signaling (Figures S3M–S3O). Most importantly only cisplatin, but not other DNA-damaging agents or the chemotherapy agent paclitaxel, induced dissociation of cRaf-MEK1 (Figure 3M). In line with this dissociation, knockdown of MAST1 only enhanced sensitivity to cisplatin but not to other DNA-damaging agents or paclitaxel (Figures 3N and S3P). These data together suggest that MAST1 contributes to cisplatin-resistant cell survival not by acting as a critical element of the DNA-damage response but by activating MEK-mediated anti-apoptotic signaling.

We next investigated whether MEK1, as a downstream phosphorylation target of MAST1, contributes to MAST1-dependent pro-survival signals in response to cisplatin. Cancer cell lines with stable knockdown of MAST1 and forced expression of phospho-mimetic (S221D) or phospho-deficient (S221A) mutant of MEK1 were generated and examined for proliferative potential *in vitro* and *in vivo* (Figure 4A). Silencing MAST1 using shRNA did not affect cell viability and apoptosis induction in the absence of cisplatin. But with cisplatin treatment, knockdown of MAST1 significantly decreased cell viability and enhanced apoptosis induction, whereas expression of S221D, but not S221A, MEK1 significantly rescued the phenotypes resulting from MAST1 knockdown (Figures 4B and 4C). Furthermore, S221D but not S221A MEK1 restored the attenuated tumor growth of MAST1 knockdown KB-3-1^{cisR} xenografts treated

Figure 3. Cisplatin but No Other DNA-Damaging Agents Dissociates cRaf from MEK1 and Reactivates MEK1 through MAST1

- (A) Interaction between cRaf and MEK1 upon cisplatin treatment in diverse cancer types. Cells were treated with 5 $\mu\text{g}/\text{mL}$ cisplatin for 24 hr prior to MEK1 immunoprecipitation.
- (B) Purified MEK1-cRaf complex from KB-3-1 cells were incubated with increasing concentrations of cisplatin (0–5 $\mu\text{g}/\text{mL}$) for 2 hr and applied to western blotting.
- (C) Biacore SPR (left) and thermal shift assay (right) were performed using purified recombinant MEK1 or cRaf with increasing concentrations of cisplatin.
- (D) MAST1 interacts with cRaf and MEK1 in cancer cells. ov, overexpressed.
- (E) Dissociation constant (K_D) values for MEK1-cRaf or MEK1-MAST1 interaction in the presence and absence of cisplatin were determined by Biacore SPR analysis.
- (F) Interactions between MEK1 variants and cisplatin or cRaf in the absence and presence of cisplatin were determined by SPR and shown as K_D values. N.D., not determined.
- (G) Binding affinity of WT and C142A MEK1 to cRaf in the presence of cisplatin. MEK1 shRNA-resistant FLAG-MEK1 WT and C142A were expressed in MEK1 knockdown KB-3-1 cells. Cells were treated with cisplatin (5 $\mu\text{g}/\text{mL}$) for the indicated time and MEK1-cRaf interaction was determined by flag pull-down.
- (H) Effect of cRaf (top) or MAST1 (bottom) downregulation on MEK1 activation in the presence and absence of cisplatin. cRaf and MAST1 knockdown cells were treated with cisplatin for 48 hr and MEK1 activity was determined by p-MEK S217/S221 western blotting.
- (I) Effect of MAST1 rescue expression on MEK1 activation in MAST1 knockdown cells with cisplatin treatment.
- (J) Effect of WT or DA MAST1 expression on MEK1 activation in cRaf knockdown cells in the presence or absence of cisplatin.
- (K) Purified MEK1-cRaf complex from KB-3-1 cells were incubated with 5 $\mu\text{g}/\text{mL}$ cisplatin. Samples were collected at different time points and subjected to immunoblotting. Density analysis of relative amount of cRaf bound to MEK1 from three biological replicates is shown.
- (L) Accumulation of cisplatin-induced DNA damage and repair in KB-3-1 cells with or without MAST1 shRNA was determined by flow-cytometry analysis of phospho- γH2AX (upper) and phospho-53BP1 (lower). For DNA repair, cells were treated with cisplatin (5 $\mu\text{g}/\text{mL}$) for 2 hr before cisplatin was washed off and cells were incubated in fresh medium.
- (M) cRaf-MEK1 dissociation induced by DNA-damaging agents and cytotoxic drugs. KB-3-1 cells were treated with different compounds as indicated, followed by MEK1 immunoprecipitation and immunoblotting.
- (N) Cells with or without MAST1 knockdown were treated with different concentrations of DNA-damaging agents and cytotoxic drugs and IC_{50} values were obtained.

Error bars represent $\pm\text{SD}$ from three biological (K) or technical (L) replicates. p values were determined by two-tailed Student's t test (ns, not significant). See also Figure S3.

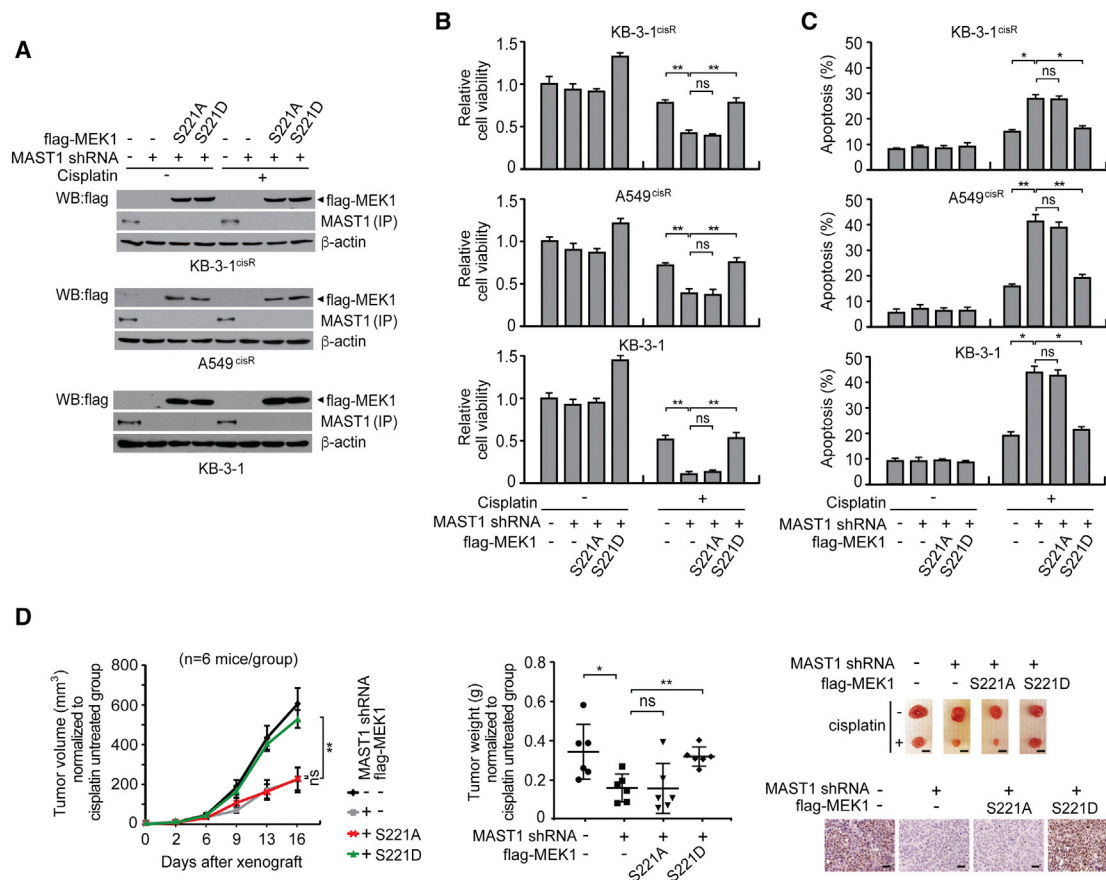


Figure 4. MAST1 Induces Cisplatin-Resistant Cancer Cell Proliferation and Tumor Growth through MEK1 Phosphorylation

(A) MAST1 and FLAG-tagged S221A and S221D MEK1 expression were detected by immunoblotting in KB-3-1^{cisR}, A549^{cisR}, and KB-3-1 cells.

(B and C) Cell viability (B) and apoptosis (C) in MAST1 knockdown cells with the expression of the indicated MEK1 variants in the presence and absence of sublethal dose of cisplatin (2 μg/mL, parental; 5 μg/mL, cis^R).

(D) Tumor volume (left), tumor weight (middle), and Ki-67 expression (right) of KB-3-1^{cisR} cell xenograft mice. Representative dissected tumors are shown on right top panel. KB-3-1^{cisR} cells with MAST1 knockdown and MEK1 S221A or S221D expression were injected and cisplatin was administered by intraperitoneal injection when there were palpable tumors. Tumor volume and tumor weight were normalized to the corresponding non-cisplatin-treated group. Scale bars represent 5 mm for dissected tumors and 20 μm for Ki-67 IHC staining images.

Data are mean ± SD from three technical replicates for (B) and (C). Error bars represent SEM for tumor growth and SD for tumor weight in (D). p values were determined by two-tailed Student's t test (ns: not significant; *0.01 < p < 0.05; **p < 0.01).

with cisplatin (Figure 4D). These results suggest that MAST1 signals through MEK1 by phosphorylation at serine 221 to promote cisplatin-resistant cancer cell proliferation and tumor growth.

MAST1 Expression Correlates with Cisplatin Resistance of Diverse Cancer Cell Lines and Primary Tumor Tissues

To investigate the expression of MAST1 and its relationship with cisplatin resistance in human cancer, we examined MAST1 expression and cisplatin response in 39 human cancer cell lines and 13 patient-derived xenograft (PDX) HNSCC, lung cancer, and ovarian cancer tissues (Geisinger et al., 1989; Lin et al., 2007). We found that MAST1 expression positively correlates with cisplatin IC₅₀ (Figures 5A–5D, S4A, and S4B). Knockdown of MAST1 by shRNA sensitized diverse cancer cells to cisplatin, while overexpression of WT but not DA MAST1 conferred cisplatin resistance to these cells (Figure 5E). We found that MAST1 expression levels, both protein and mRNA, were upregu-

lated in cisplatin-resistant (cis^R) cells that were chronically exposed to cisplatin, compared with parental cells (Figure S4C). Furthermore, we observed increased correlation between MAST1 and MEK phosphorylation in cisplatin-treated cells compared with non-treated cells (Figure S4D).

To demonstrate the clinical relevance of our findings, we evaluated MAST1 and phospho-MEK levels in 97 HNSCC patient cases who received platinum-containing therapy or non-platinum-based therapy such as radiation or surgery (Figures 6A, S5A, and S5B; Tables S1 and S2). For cases of platinum-containing therapy, patients who showed no evidence of disease for over 2 years after chemotherapy with cisplatin and/or carboplatin were considered “Sensitive” and patients with disease recurrence within 2 years were considered “Resistant.” To determine whether a high MAST1 level initially and after the chemotherapy confers cisplatin resistance, we analyzed MAST1 and phospho-MEK levels in tumor samples collected before and after platinum-containing chemotherapy. The

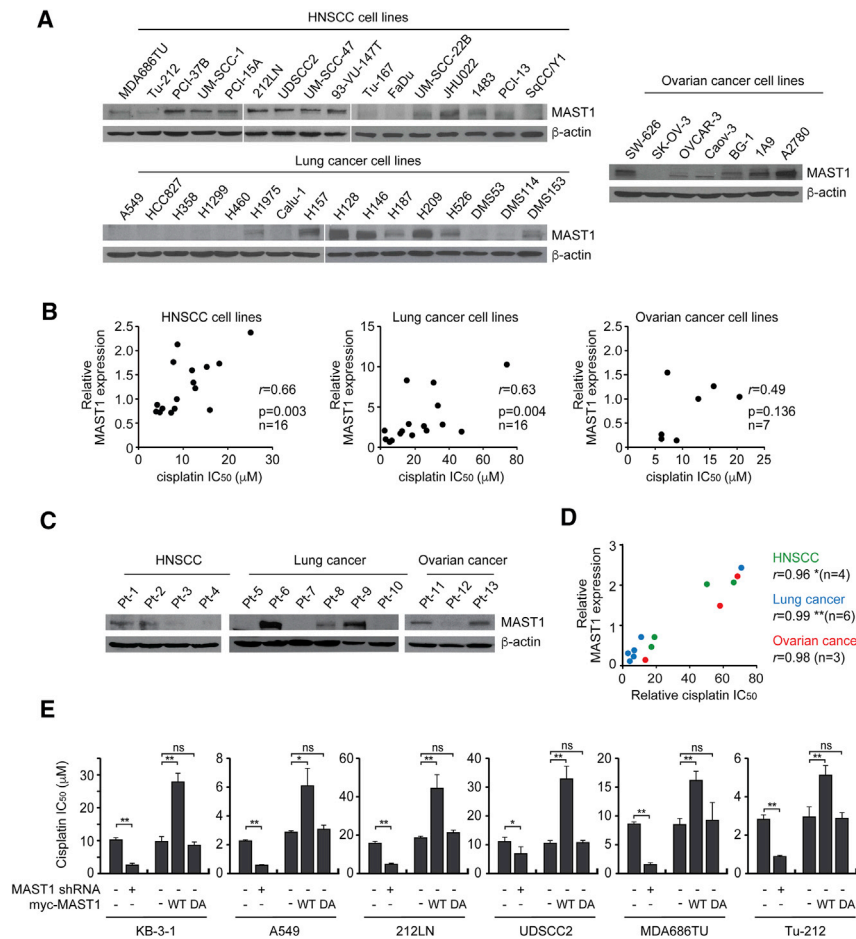


Figure 5. MAST1 Expression Correlates with Cisplatin Resistance in Cancer Cell Lines and Patient-Derived Tumors

(A) MAST1 expression in HNSCC, lung, and ovarian cancer cell lines. (B) Correlation between MAST1 expression and cisplatin IC₅₀ in cancer cell lines shown in (A). (C) MAST1 expression in PDX tumors. (D) Correlation between MAST1 expression and cisplatin IC₅₀ in PDX tumors shown in (C). *r*, Pearson's correlation coefficient. (E) Effect of MAST1 knockdown or WT or DA MAST1 overexpression on cisplatin response in diverse cancer cell lines. Cisplatin response was determined using cisplatin IC₅₀. Error bars represent SD from three technical replicates. *p* values were determined by two-tailed Student's *t* test (ns, not significant; *0.01 < *p* < 0.05; ***p* < 0.01). See also Figure S4.

therapy (long term), which together leads to platinum resistance and worse clinical outcome.

Identification and Characterization of Lestaurtinib as a MAST1 Inhibitor to Target Cisplatin-Resistant Cancer

Our finding that MAST1 is upregulated in cisplatin-resistant cancer and that attenuation of MAST1 sensitizes cancer cells to cisplatin treatment implicates MAST1 as a promising anti-cancer target to overcome cisplatin resistance. To our knowl-

edge, there is no compound reported as a MAST1 inhibitor. We thus screened for a MAST1 inhibitor by testing the top ten small molecules among 72 kinase inhibitors documented to bind to MAST1 (Figure 7A), according to the IUPHAR database, which provides binding reactivity of the 72 inhibitors against 456 kinases (Davis et al., 2011). Six inhibitors out of 10 that showed a significant decrease in MAST1 activity were evaluated for their ability to sensitize cancer cells to cisplatin-induced cell death (Figure 7B). MAST1 inhibition efficacy strongly correlated with cisplatin response with an *r* value of 0.82 (Figure 7C). Among these, lestaurtinib sensitized cells to cisplatin treatment the most using a concentration that attenuates cell viability by less than 20% when treated alone. Lestaurtinib effectively inhibited MAST1 *in vitro* and in cells (Figure 7D). We also showed that lestaurtinib inhibits MAST1 as an ATP competitive inhibitor (Figure 7E). To demonstrate the selectivity of lestaurtinib binding to MAST1, we generated a MAST1 L504D mutant. Leucine 504 in MAST1 is predicted to be critical for lestaurtinib binding based on the structure of lestaurtinib and PRK1, a kinase that has a catalytic domain similar to that of MAST1 (Chamberlain et al., 2014). Cellular thermal shift assay showed that MAST1 L504D no longer binds to lestaurtinib (Figure 7F). Lestaurtinib attenuated the kinase activity of WT but not L504D MAST1 (Figure 7G). In line with the kinase activity, lestaurtinib did not sensitize cells to cisplatin when

Resistant group showed significantly higher MAST1 and phospho-MEK1 levels compared with the Sensitive group in both pre- and post-treatment tumor samples (Figures 6B and S5C). In support of our finding that cisplatin drives MAST1-mediated MEK activation, significant positive correlations between MAST1 and phospho-MEK levels were observed in post-platinum treatment samples, but not in samples collected before the treatment (Figure 6C). To determine whether MAST1 is induced during platinum treatment, we evaluated pre- and post-treatment samples. Analysis of pre- and post-treatment paired tumor samples obtained from individual patients showed that MAST1 staining increased after cisplatin treatment, whereas this increase was not observed in paired samples collected from cancer patients who received regimens other than platinum-based therapy (Figures 6D and S5D). Similar to paired tumors, the analysis of non-paired pre- and post-treatment tumors also demonstrated that MAST1 was higher after platinum-based therapy, but not after non-platinum-based therapy (Figure 6E). Furthermore, high MAST1 expression was associated with a worse clinical outcome in cancer patients who received platinum-containing chemotherapy, but not in cancer patients who received non-platinum-based therapy (Figures 6F and 6G). Collectively, these results illustrate that initial MAST1 expression significantly correlates with platinum resistance (short term), and that MAST1 is further induced during platinum-based chemo-

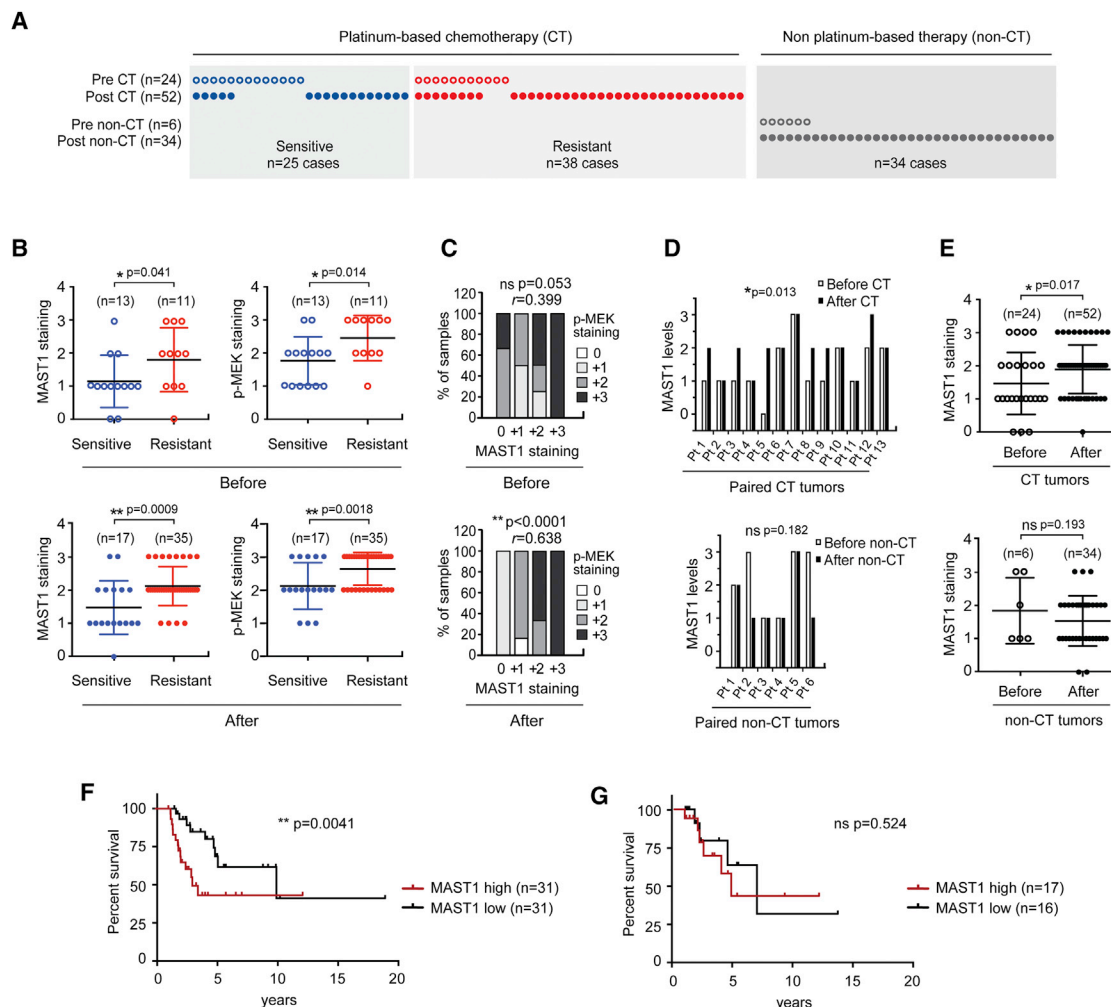


Figure 6. MAST1 and MEK Activation Is Associated with Cisplatin Resistance and Poor Clinical Outcome in Human HNSCC

(A) Schematic summary of HNSCC patients (n = 97 cases) and samples (n = 116 tumors) analyzed by IHC staining. Open circles, pre-therapy tumors; closed circles, post-therapy tumors. Tumor numbers of before or after CT or non-CT groups are indicated on the left. Case numbers for sensitive or resistant CT or non-CT treated patients are indicated at the bottom. CT, platinum-based chemotherapy.

(B) MAST1 expression and MEK phosphorylation levels and drug response in specimens before (top) and after (bottom) platinum treatment.

(C) Correlation between MAST1 and phospho-MEK in samples before (top) and after (bottom) platinum treatment.

(D and E) Comparison of MAST1 status between pre- and post-therapy in paired (D) and non-paired (E) samples. Top: platinum therapy; bottom: non-platinum therapy.

(F and G) Kaplan-Meier survival analysis of platinum-treated (F) and non-platinum-treated (G) patient groups. Patients were dichotomized by MAST1 expression level at median.

Error bars represent \pm SD for (B) and (E). p values were determined by Pearson correlation for (C), paired Student's t test for (D), log-rank test for (F) and (G), and unpaired Student's t test for the rest (ns, not significant; *0.01 < p < 0.05; **p < 0.01). See also Figure S5.

harboring L504D MAST1, suggesting that lestaurtinib sensitizes cells to cisplatin by binding and inhibiting MAST1 kinase activity (Figure 7H). Overexpression of MAST1 enhanced cisplatin resistance and MEK activation but had no impact on cRaf activity in various cell lines with different cisplatin sensitivity, whereas 100 nM lestaurtinib was sufficient to fully inhibit both endogenous and overexpressed MAST1 in these cells, suggesting that the drug capacity is high enough to inhibit any excessive MAST1 in cells (Figures 7I, S6A, and S6B). Lestaurtinib was not effective in cells overexpressing L504D MAST1, further supporting that the drug's effect on cisplatin response and MEK activation is through MAST1 inhibition. Furthermore,

lestaurtinib sensitizes cells to cisplatin treatment in diverse cell lines, while the effect was abolished in MAST1 knockdown cells *in vitro* and *in vivo* (Figures 7J–7M and S6C–S6G). Lestaurtinib is a tyrosine kinase inhibitor known to inhibit FLT3, JAK2, Trk, and PRK1 (Shabbir and Stuart, 2010). Other known FLT3, Trk, or JAK2 inhibitors did not alter cisplatin sensitivity in cancer cells (Figure S6H). Furthermore, FLT3 and Trk were not expressed in the cancer cells we tested, and genetic inhibition of JAK2 did not alter cisplatin response (Figures S6I and S6J). These data together suggest that cisplatin sensitivity conferred by lestaurtinib occurs mainly through MAST1 inhibition, not through other kinases.

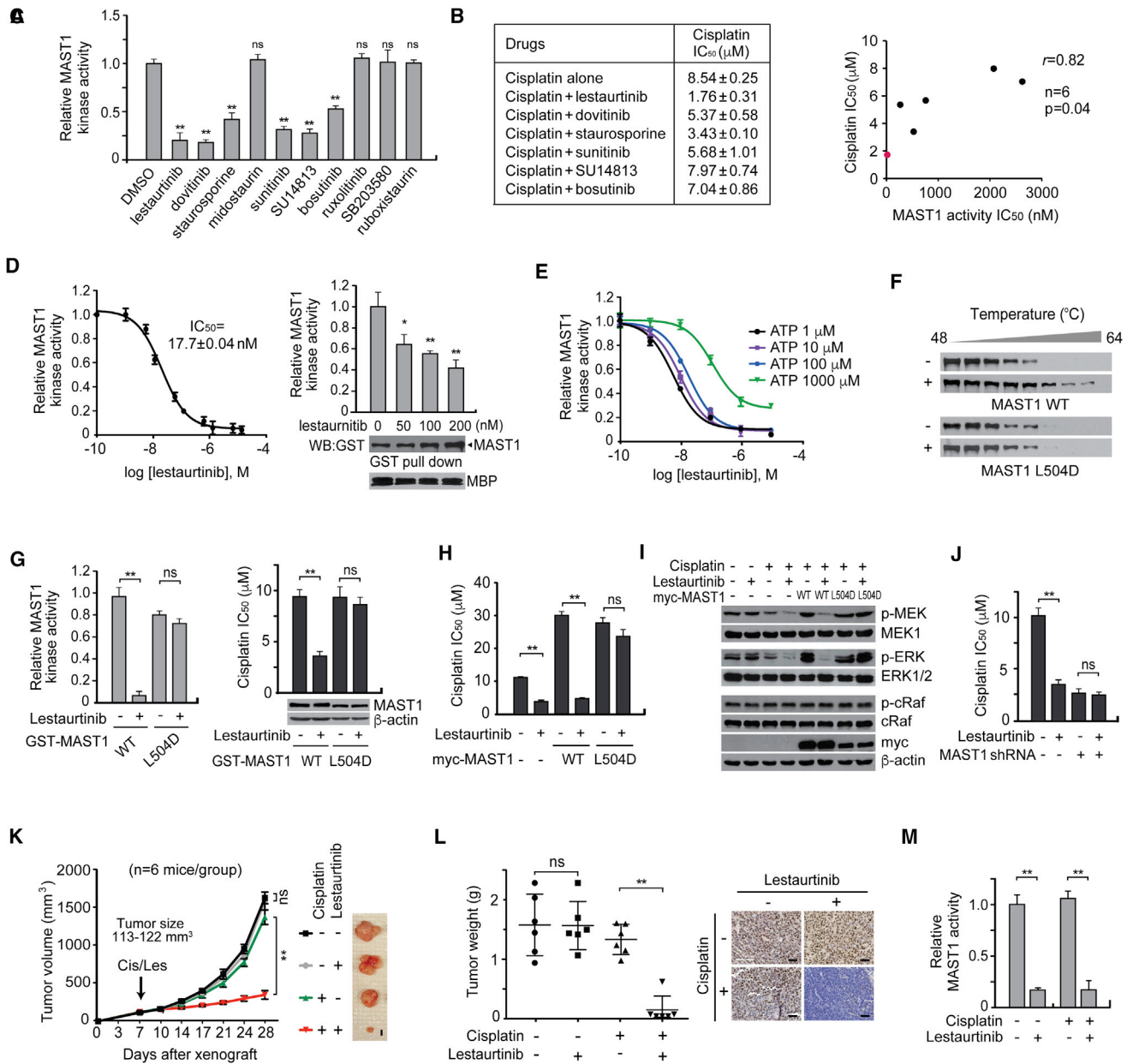


Figure 7. Validation of Lestaurnitinib as a MAST1 Inhibitor

(A) *In vitro* MAST1 kinase assay using ten compounds potentially bind to MAST1. Compounds (10 μM) were incubated with purified GST-MAST1 and applied to the *in vitro* kinase assay.

(B) Effect of top six MAST1 inhibitors from (A) on cisplatin sensitivity in KB-3-1 cells. A dose of inhibitor that did not affect viability when given alone (100 nM lestaurnitinib, dovitinib, staurosporine; 1 μM sunitinib, SU14813, bosutinib) was used with increasing concentrations of cisplatin for 48 hr.

(C) Correlation between MAST1 activity inhibition and cisplatin sensitivity of the top six MAST1 inhibitors. Red indicates lestaurnitinib.

(D) Effect of lestaurnitinib on MAST1 activity *in vitro* (left) and *in vivo* in KB-3-1 cells (right). Purified GST-MAST1 variants were treated with increasing concentrations of lestaurnitinib.

(E) Effect of lestaurnitinib on MAST1 activity at a range of ATP concentrations.

(F) Cellular thermal shift assay using KB-3-1 cells harboring WT or L504D MAST1 treated without (–) or with (+) lestaurnitinib.

(G) Kinase activity of MAST1 WT or L504D treated with lestaurnitinib.

(H) Cisplatin IC₅₀ upon lestaurnitinib treatment in KB-3-1 cells with endogenous MAST1 knockdown expressing MAST1 WT or L504D in KB-3-1 cells.

(I) Effect of lestaurnitinib and WT or L504D MAST1 overexpression on MEK and cRaf phosphorylation in KB-3-1 cells.

(J) Cisplatin IC₅₀ upon lestaurnitinib treatment in cells with or without MAST1 knockdown in KB-3-1 cells.

(K) Tumor growth of lestaurnitinib and cisplatin-treated mice carrying KB-3-1^{cisR} cell xenografts. Error bars represent SEM. Representative tumors for each group are shown. Scale bar represents 5 mm.

(legend continued on next page)

Finally, we evaluated the efficacy of lestaurtinib in abrogating cisplatin resistance *in vitro* and *in vivo*. Treatment of lestaurtinib effectively sensitized multiple cis^S and cis^R cells to not only cisplatin (Figure S7A) but also carboplatin (Figure S7B). Furthermore, lestaurtinib and cisplatin synergistically attenuated cell viability in cells with combination index (CI) of around 0.26 (Figure 8A, left). In KB-3-1 cells, lestaurtinib alone partially decreased cell viability, and apparently this was not due to increased apoptosis. Similar results were obtained in colony-formation assays (Figure 8A, middle). Consistent with the phenotype observed in MAST1 knockdown cells, inhibition of MAST1 by lestaurtinib in combination with cisplatin resulted in increased apoptotic cell death and decreased MEK activation (Figure 8A, right). Similar results were obtained in multiple cis^S and cis^R cells (Figure S6B). In addition, combination of lestaurtinib and cisplatin synergistically attenuated cell viability in primary platinum-refractory TKO-002 cells with CI value of 0.57 (Figure 8B). Consistent with MAST1 knockdown, targeting MAST1 with lestaurtinib sensitized cells to cisplatin but not to other DNA-damaging agents or chemotherapy agents, further supporting that the synergistic effect of MAST1 inhibition is specific to cisplatin (Figure S7C). Moreover, the effect of lestaurtinib was greater in cell lines and patient-derived tumors with higher MAST1 levels (Figures S7D and S7E). Lastly, we established PDX models using diverse cancer patient tumors including HNSCC, lung cancer, and ovarian cancer. The dosage of 20 mg/kg lestaurtinib and 5 mg/kg cisplatin did not induce significant changes in body weight, histopathology, or hematopoietic properties (Figures S8A–S8C). The combination significantly reduced PDX tumor growth and tumor cell proliferation compared with single-agent treatment (Figures 8C and 8D). Moreover, a higher dose of lestaurtinib (30 mg/kg) achieved better efficacy in inhibiting MAST1 activity and tumor growth (Figure S8D). Lestaurtinib significantly attenuated MAST1 activity and MEK/ERK phosphorylation but not Ras or Raf activity in PDX tumors (Figures 8E, 8F, S8E, and S8F). Finally, to demonstrate whether the effect of MAST1 inhibitor lestaurtinib on the response to cisplatin therapy is mediated through MEK, we compared the effect of an MEK inhibitor on enhancing cisplatin therapy with that of lestaurtinib *in vitro* and *in vivo* in an additional PDX model of lung cancer. The combination of trametinib and cisplatin mimicked the lestaurtinib and cisplatin effect resulting in cisplatin sensitization and attenuated PDX tumor growth and proliferation, but lestaurtinib showed a slightly greater synergistic effect than trametinib or AZD6244 (Figures S8G–S8K). These results together suggest that the MAST1-MEK1 signaling axis is a crucial pathway for cancer cisplatin resistance and that lestaurtinib is a MAST1 inhibitor with promising anti-tumor effect in combination therapy with cisplatin in human cancers.

DISCUSSION

Here we identify MAST1 as a synthetic lethal partner of cisplatin that functions as a critical factor to program cisplatin-resistant

pro-survival signaling in human cancers. Our findings suggest a mechanistic basis by which MAST1 controls cancer cells to evade cisplatin-induced cell death. Cells predominantly depend on Raf for MEK1 activation during active cell proliferation (Lavoie and Therrien, 2015). Consistently we found that, although MAST1 is present in the cRaf-MEK1 complex, cancer cells depend on cRaf-dependent MEK1 activation to promote proliferation and tumor growth (Figure 8G, left). However, cisplatin treatment dissociates cRaf from MEK1, whereas MAST1 remains in complex with MEK1. MAST1 phosphorylates MEK1, leading to cRaf-independent activation of MEK1 and the downstream MAPK pathway including loss of the pro-apoptotic BIM. This MAST1-mediated MEK1 activation provides anti-apoptotic and proliferative protection to cancer cells treated with cisplatin, which, if sufficient to reverse the pro-apoptotic signaling induced by cisplatin, promotes cancer cell proliferation and tumor growth (Figure 8G, right). Our studies using clinical samples support that upregulation of MAST1 positively correlates with non-response to platinum therapy. There may exist two complementary paths to MAST1-mediated platinum resistance, which are initially high levels of MAST1 and the ability to upregulate MAST1 in response to platinum.

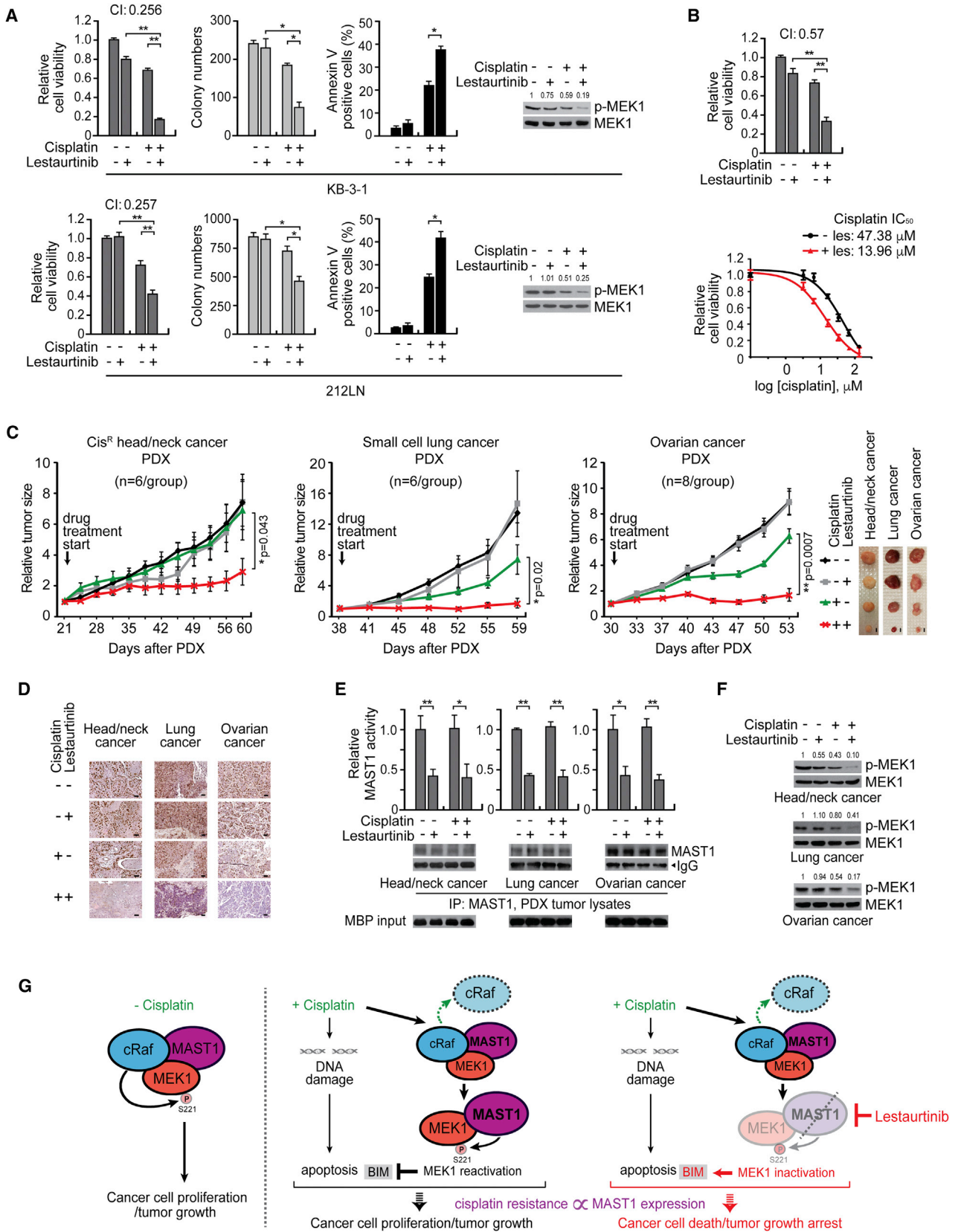
Our study provides evidence that cisplatin inactivates the MAPK pathway by dissociating cRaf from MEK1, while MAST1 reactivates the MAPK pathway. Characterization of the DNA-damage response upon MAST1 loss and demonstration of the specificity of the MAST1 effect for cisplatin but not broadly for DNA-damaging drugs reveals that targeting MAST1 may be impactful specifically for cisplatin therapy. The specific structure of cisplatin may disrupt the MEK1-cRaf complex, resulting in MAST1 as the sole kinase remaining in the complex. Previous reports showed that cRaf binding sites in MEK1 consist of Ser217/Ser221, whereas predicted cisplatin binding sites in MEK1 are Met56 and Cys104 (Caunt et al., 2015; Yamamoto et al., 2015). We revealed that cisplatin directly binds to MEK1 but not cRaf. We also found that MEK1 and cRaf dissociates in the presence of cisplatin, whereas the binding affinity of MEK1 and MAST1 is unaltered or slightly increased by cisplatin. It is possible that cisplatin binds to MEK1 and induces conformational changes that affect cRaf but not MAST1 binding. Since MAST1 remains within the complex while cRaf dissociates from MEK1 upon cisplatin treatment, cisplatin may not be involved in MAST1 recruitment or MAST1 binding to MEK1. Future mutational and structural studies are warranted to determine the structural mechanisms by which cisplatin affects cRaf and MAST1 function.

Since the dissociation of cRaf from MEK1 induces MAST1 to reactivate the MAPK pathway, any cellular events that affect cRaf-MEK1 binding may activate MAST1-dependent MEK1 activation. Indeed, our result showed that cRaf knockdown in the absence of cisplatin is sufficient to induce MAST1-dependent MEK1 activation, suggesting that MAST1 might represent an alternative upstream kinase of MEK1 that activates the MAPK pathway. In fact, a similar “kinase switch” has been observed in cells. MEK1 can be activated by several alternative kinases such as MEKK1, Mos in oocytes, and Cot1 or MLK in melanoma,

(L) Tumor weight (left) and Ki-67 IHC staining (right) at the experimental endpoint. Error bars represent SD. Scale bars represent 50 μ m.

(M) MAST1 activities in tumor lysates are shown.

Data are mean \pm SD from three replicates of each sample except (K) and (L). p values were determined by two-tailed Student's t test (ns, not significant; *0.01 < p < 0.05; **p < 0.01). See also Figure S6.



(legend on next page)

bypassing Raf as one mechanism of resistance to BRAF inhibitors (Gardner et al., 1994; Johannessen et al., 2010; Marusiak et al., 2014; Verhac et al., 2000). Although the MAPK pathway is implicated in cisplatin resistance, the detailed mechanism underlying its role is still unclear (Kong et al., 2015; Wang and Wu, 2014). Our findings reveal a mechanism by which a kinase MAST1-mediated cRaf-independent reactivation of the MAPK pathway contributes to the development of cisplatin resistance.

MAST1 appears to interact with syntrophin and links the dystrophin/utrophin network with microtubule filaments in cells. No disorders are reported to be associated with the MAST1 gene, and only a few studies reveal links between MAST family members and human cancer. For instance, MAST2 is known to bind and phosphorylate the tumor suppressor PTEN (phosphatase and tensin homolog) (Valiente et al., 2005). Robinson et al. demonstrated recurrent rearrangements involving MAST1 and MAST2 encoding genes in breast cancer, and overexpression of MAST1 or MAST2 gene fusions had proliferative effects (Robinson et al., 2011). Interestingly, two out of three identified MAST1 fusion genes lack its serine/threonine kinase domain-coding region, suggesting that a kinase-independent role of MAST1 may exist that contributes to proliferative potential in cancer. However, our data illustrate that kinase activity of MAST1 is required for cisplatin resistance.

From a clinical perspective, our findings support that MAST1 could serve as a predictive marker and as a promising therapeutic target to treat cancer patients in combination with platinum-based chemotherapy. We identified lestaurtinib as a potent MAST1 inhibitor with promising cisplatin-sensitization potential. Although lestaurtinib was originally reported as a tyrosine kinase inhibitor that inhibits FLT3 as well as JAK2 and Trk (Shabbir and Stuart, 2010), it has been suggested that many multi-kinase inhibitors target both serine/threonine and tyrosine kinases (Bilanges et al., 2008; Dawson et al., 2010; Garcia-Manero et al., 2015). Consistent with this concept, we demonstrate that lestaurtinib effectively inhibits the serine/threonine kinase MAST1. Our findings that other FLT3, JAK2, and Trk inhibitors did not confer cisplatin sensitization and lestaurtinib had no effect on cisplatin response in cells deficient in MAST1 suggest that MAST1 represents the primary target through which lestaurtinib sensitizes cancer cells to cisplatin. Lestaurtinib is generally well tolerated in patients (Knapper et al., 2006) and is currently under clinical evaluation. We validated the efficacy of lestaurtinib in

abolishing cisplatin resistance in PDXs of diverse cancers, which suggests that our approach could be commonly applied to treat various types of cancers. MAST1-targeted therapy would be more beneficial to patients with advanced cancers or patients who received platinum-based therapy but recurred, in part, due to the induction of MAST1 during the treatment. Future pharmacokinetics and toxicity studies, and clinical trials, are warranted to evaluate and optimize dose and treatment conditions for the proposed anti-MAST1 therapy.

STAR★METHODS

Detailed methods are provided in the online version of this paper and include the following:

- KEY RESOURCES TABLE
- CONTACT FOR REAGENT AND RESOURCE SHARING
- EXPERIMENTAL MODEL AND SUBJECT DETAILS
 - Human Studies
 - Animal Studies
 - Cell Culture
- METHOD DETAILS
 - RNAi Screens
 - Virus Production and Infection for Protein Overexpression in Cancer Cells
 - Cell Viability Assay, Colony Formation Assay, and Apoptosis Assay
 - Kinase Activity Assays
 - Cisplatin or Carboplatin Sensitivity Assay
 - Phospho-Protein Profiling
 - Surface Plasmon Resonance (SPR)
 - Thermal Shift Assay
 - MicroScale Thermophoresis (MST)
 - Immunohistochemical Staining
 - Xenograft Studies
 - Cellular Thermal Shift Assay
- QUANTIFICATION AND STATISTICAL ANALYSIS
- DATA AND SOFTWARE AVAILABILITY

SUPPLEMENTAL INFORMATION

Supplemental Information includes eight figures and two tables and can be found with this article online at <https://doi.org/10.1016/j.ccell.2018.06.012>.

Figure 8. Lestaurtinib Sensitizes Cancer Cells to Cisplatin Treatment *In Vitro* and *In Vivo*

(A) Cell viability, colony formation, apoptosis induction, and MEK1 phosphorylation in KB-3-1 and 212LN with vehicle control, lestaurtinib, cisplatin, and the combination.

(B) Lestaurtinib effect on cell viability and cisplatin sensitivity of TKO-002 cells. Combination index (CI) values for synergistic effect are shown.

(C) Effect of lestaurtinib, cisplatin and the combination effect on tumor growth of cis^R HNSCC, lung cancer, and ovarian cancer PDX mice. Pt-8 tumor and Pt-11 tumor in Figure 5C were used for lung cancer PDX and ovarian cancer PDX, respectively. Error bars represent SEM. Scale bars for the dissected tumors represent 5 mm.

(D) Ki-67 expression was determined by IHC staining. Scale bars represent 50 μ m.

(E) MAST1 activity was assessed by MAST1 *in vitro* kinase assay using MBP as a substrate.

(F) MEK1 inhibition by lestaurtinib and cisplatin combination in PDX tumor lysates.

(G) Proposed model for the role of MAST1 in cisplatin resistance in human cancer. Left: cancer cells rely on cRaf-dependent MEK1 activation to promote tumor growth in the absence of cisplatin. Right: cisplatin treatment dissociates cRaf from MEK1, while MAST1 phosphorylates MEK1 to activate the MAPK pathway in cRaf-independent manner, inhibiting BIM and providing a proliferative advantage to cancer cells. Targeting MAST1 by lestaurtinib restores cisplatin sensitivity to cells.

Data are mean \pm SD from three technical replicates of each sample except (C). p values were determined by two-tailed Student's t test (*0.01 < p < 0.05; **p < 0.01). See also Figures S7 and S8.

ACKNOWLEDGMENTS

We acknowledge Dr. Anthea Hammond for editorial assistance. We thank Thomas Schubert and Maximilian Plach at 2bind, Germany for performing microscale thermophoresis assay. ICP-mass spectrometry was performed at the Center for Applied Isotope Studies, University of Georgia. This work was supported in part by NIH grants R01 CA175316 (S.K.), R01 CA207768 (S.K.), F31 CA183365 (G.A.), DoD grant W81XWH-17-1-0186 (S.K.), developmental funds from the Winship Cancer Institute of Emory University (S.K.), Winship Cancer Institute #IRG-17-181-04 from the American Cancer Society (L.J.), and the Emory University Integrated Cellular Imaging Microscopy Core of the Winship Cancer Institute Comprehensive Cancer Center grant, P30CA138292. G.A. is an NIH pre-doctoral fellow. J.K., F.R.K., and S.K. are Georgia Cancer Coalition Scholars. S.K. is a Robbins Scholar and an American Cancer Society Basic Research Scholar.

AUTHOR CONTRIBUTIONS

S.L., T.K.O., C.-K.Q., L.H.B., F.R.K., G.Z.C., and N.F.S. provided critical reagents. L.Z. and T.J.B. performed structural analyses. K.R.M. collected clinical samples and performed histopathological study. H.-B.K. generated kinome shRNA lentivirus. D.W. and G.Z. performed patient-derived xenografting. J.K. performed biostatistical study. X.W., C.E.S., and D.M.S. provided clinical information. L.J., J.C., C.P., D.L., J.F., R.L., L.S., and G.N.A. performed all other experiments. L.J. and S.K. designed the study and wrote the paper.

DECLARATION OF INTERESTS

The authors declare no competing interests.

Received: September 15, 2017

Revised: March 12, 2018

Accepted: June 21, 2018

Published: July 19, 2018

REFERENCES

Aida, T., Takebayashi, Y., Shimizu, T., Okamura, C., Higashimoto, M., Kanzaki, A., Nakayama, K., Terada, K., Sugiyama, T., Miyazaki, K., et al. (2005). Expression of copper-transporting P-type adenosine triphosphatase (ATP7B) as a prognostic factor in human endometrial carcinoma. *Gynecol. Oncol.* **97**, 41–45.

Bilanges, B., Torbett, N., and Vanhaesebroeck, B. (2008). Killing two kinase families with one stone. *Nat. Chem. Biol.* **4**, 648–649.

Caunt, C.J., Sale, M.J., Smith, P.D., and Cook, S.J. (2015). MEK1 and MEK2 inhibitors and cancer therapy: the long and winding road. *Nat. Rev. Cancer* **15**, 577–592.

Chamberlain, P., Delker, S., Pagarigan, B., Mahmoudi, A., Jackson, P., Abbasian, M., Muir, J., Raheja, N., and Cathers, B. (2014). Crystal structures of PRK1 in complex with the clinical compounds lestaurtinib and tofacitinib reveal ligand induced conformational changes. *PLoS One* **9**, e103638.

Datta, S.R., Dudek, H., Tao, X., Masters, S., Fu, H., Gotoh, Y., and Greenberg, M.E. (1997). Akt phosphorylation of BAD couples survival signals to the cell-intrinsic death machinery. *Cell* **91**, 231–241.

Davis, M.I., Hunt, J.P., Herrgard, S., Ciceri, P., Wodicka, L.M., Pallares, G., Hocker, M., Treiber, D.K., and Zarrinkar, P.P. (2011). Comprehensive analysis of kinase inhibitor selectivity. *Nat. Biotechnol.* **29**, 1046–1051.

Dawson, M.A., Curry, J.E., Barber, K., Beer, P.A., Graham, B., Lyons, J.F., Richardson, C.J., Scott, M.A., Smyth, T., Squires, M.S., et al. (2010). AT9283, a potent inhibitor of the Aurora kinases and Jak2, has therapeutic potential in myeloproliferative disorders. *Br. J. Haematol.* **150**, 46–57.

Fijolek, J., Wiatr, E., Rowinska-Zakrzewska, E., Giedronowicz, D., Langfort, R., Chabowski, M., Orlowski, T., and Roszkowski, K. (2006). p53 and HER2/neu expression in relation to chemotherapy response in patients with non-small cell lung cancer. *Int. J. Biol. Markers* **27**, 81–87.

Gad, H., Koolmeister, T., Jemth, A.S., Eshtad, S., Jacques, S.A., Strom, C.E., Svensson, L.M., Schultz, N., Lundback, T., Einarsdottir, B.O., et al. (2014).

MTH1 inhibition eradicates cancer by preventing sanitation of the dNTP pool. *Nature* **508**, 215–221.

Galanski, M. (2006). Recent developments in the field of anticancer platinum complexes. *Recent Pat. Anticancer Drug. Discov.* **1**, 285–295.

Garcia-Manero, G., Khoury, H.J., Jabbour, E., Lancet, J., Winski, S.L., Cable, L., Rush, S., Maloney, L., Hogeland, G., Ptaszynski, M., et al. (2015). A phase I study of oral ARRY-614, a p38 MAPK/Tie2 dual inhibitor, in patients with low or intermediate-1 risk myelodysplastic syndromes. *Clin. Cancer Res.* **21**, 985–994.

Gardner, A.M., Vaillancourt, R.R., Lange-Carter, C.A., and Johnson, G.L. (1994). MEK-1 phosphorylation by MEK kinase, Raf, and mitogen-activated protein kinase: analysis of phosphopeptides and regulation of activity. *Mol. Biol. Cell* **5**, 193–201.

Garland, P., Quraisha, S., French, P., and O'Connor, V. (2008). Expression of the MAST family of serine/threonine kinases. *Brain Res.* **1195**, 12–19.

Geisinger, K.R., Kute, T.E., Pettenati, M.J., Welander, C.E., Dennard, Y., Collins, L.A., and Berens, M.E. (1989). Characterization of a human ovarian carcinoma cell line with estrogen and progesterone receptors. *Cancer* **63**, 280–288.

Giaccone, G. (2000). Clinical perspectives on platinum resistance. *Drugs* **59** (Suppl 4), 9–17, discussion 37–18.

Han, J.Y., Hong, E.K., Choi, B.G., Park, J.N., Kim, K.W., Kang, J.H., Jin, J.Y., Park, S.Y., Hong, Y.S., and Lee, K.S. (2003). Death receptor 5 and Bcl-2 protein expression as predictors of tumor response to gemcitabine and cisplatin in patients with advanced non-small-cell lung cancer. *Med. Oncol.* **20**, 355–362.

Ikeguchi, M., and Kaibara, N. (2001). Changes in survivin messenger RNA level during cisplatin treatment in gastric cancer. *Int. J. Mol. Med.* **8**, 661–666.

Johannessen, C.M., Boehm, J.S., Kim, S.Y., Thomas, S.R., Wardwell, L., Johnson, L.A., Emery, C.M., Stransky, N., Cogdill, A.P., Barretina, J., et al. (2010). COT drives resistance to RAF inhibition through MAP kinase pathway reactivation. *Nature* **468**, 968–972.

Kang, S., Elf, S., Lythgoe, K., Hitosugi, T., Taunton, J., Zhou, W., Xiong, L., Wang, D., Muller, S., Fan, S., et al. (2010). p90 ribosomal S6 kinase 2 promotes invasion and metastasis of human head and neck squamous cell carcinoma cells. *J. Clin. Invest.* **120**, 1165–1177.

Knapper, S., Burnett, A.K., Littlewood, T., Kell, W.J., Agrawal, S., Chopra, R., Clark, R., Levis, M.J., and Small, D. (2006). A phase 2 trial of the FLT3 inhibitor lestaurtinib (CEP701) as first-line treatment for older patients with acute myeloid leukemia not considered fit for intensive chemotherapy. *Blood* **108**, 3262–3270.

Koberle, B., Tomicic, M.T., Usanova, S., and Kaina, B. (2010). Cisplatin resistance: preclinical findings and clinical implications. *Biochim. Biophys. Acta* **1806**, 172–182.

Kong, L.R., Chua, K.N., Sim, W.J., Ng, H.C., Bi, C., Ho, J., Nga, M.E., Pang, Y.H., Ong, W.R., Soo, R.A., et al. (2015). MEK inhibition overcomes cisplatin resistance conferred by SOS/MAPK pathway activation in squamous cell carcinoma. *Mol. Cancer Ther.* **14**, 1750–1760.

Lavoie, H., and Therrien, M. (2015). Regulation of RAF protein kinases in ERK signalling. *Nat. Rev. Mol. Cell Biol.* **16**, 281–298.

Li, D., Jin, L., Alesi, G.N., Kim, Y.M., Fan, J., Seo, J.H., Wang, D., Tucker, M., Gu, T.L., Lee, B.H., et al. (2013). The prometastatic ribosomal S6 kinase 2-cAMP response element-binding protein (RSK2-CREB) signaling pathway up-regulates the actin-binding protein fascin-1 to promote tumor metastasis. *J. Biol. Chem.* **288**, 32528–32538.

Liedert, B., Materna, V., Schadendorf, D., Thomale, J., and Lage, H. (2003). Overexpression of cMOAT (MRP2/ABCC2) is associated with decreased formation of platinum-DNA adducts and decreased G2-arrest in melanoma cells resistant to cisplatin. *J. Invest. Dermatol.* **121**, 172–176.

Lin, C.J., Grandis, J.R., Carey, T.E., Gollin, S.M., Whiteside, T.L., Koch, W.M., Ferris, R.L., and Lai, S.Y. (2007). Head and neck squamous cell carcinoma cell lines: established models and rationale for selection. *Head Neck* **29**, 163–188.

Lumeng, C., Phelps, S., Crawford, G.E., Walden, P.D., Barald, K., and Chamberlain, J.S. (1999). Interactions between beta 2-syntrophin and a family

- of microtubule-associated serine/threonine kinases. *Nat. Neurosci.* **2**, 611–617.
- Martinez Molina, D., Jafari, R., Ignatushchenko, M., Seki, T., Larsson, E.A., Dan, C., Sreekumar, L., Cao, Y., and Nordlund, P. (2013). Monitoring drug target engagement in cells and tissues using the cellular thermal shift assay. *Science* **341**, 84–87.
- Marusiak, A.A., Edwards, Z.C., Hugo, W., Trotter, E.W., Girotti, M.R., Stephenson, N.L., Kong, X., Gartside, M.G., Fawdar, S., Hudson, A., et al. (2014). Mixed lineage kinases activate MEK independently of RAF to mediate resistance to RAF inhibitors. *Nat. Commun.* **5**, 3901.
- Metzger, R., Leichman, C.G., Danenberg, K.D., Danenberg, P.V., Lenz, H.J., Hayashi, K., Groshen, S., Salonga, D., Cohen, H., Laine, L., et al. (1998). ERCC1 mRNA levels complement thymidylate synthase mRNA levels in predicting response and survival for gastric cancer patients receiving combination cisplatin and fluorouracil chemotherapy. *J. Clin. Oncol.* **16**, 309–316.
- Moreno-Smith, M., Halder, J.B., Meltzer, P.S., Gonda, T.A., Mangala, L.S., Rupaimoole, R., Lu, C., Nagaraja, A.S., Gharpure, K.M., Kang, Y., et al. (2013). ATP11B mediates platinum resistance in ovarian cancer. *J. Clin. Invest.* **123**, 2119–2130.
- Owonikoko, T.K., Zhang, G., Kim, H.S., Stinson, R.M., Bechara, R., Zhang, C., Chen, Z., Saba, N.F., Pakkala, S., Pillai, R., et al. (2016). Patient-derived xenografts faithfully replicated clinical outcome in a phase II co-clinical trial of arsenic trioxide in relapsed small cell lung cancer. *J. Transl. Med.* **14**, 111.
- Persons, D.L., Yazlovitskaya, E.M., and Pelling, J.C. (2000). Effect of extracellular signal-regulated kinase on p53 accumulation in response to cisplatin. *J. Biol. Chem.* **275**, 35778–35785.
- Richert, N., Akiyama, S., Shen, D., Gottesman, M.M., and Pastan, I. (1985). Multiply drug-resistant human KB carcinoma cells have decreased amounts of a 75-kDa and a 72-kDa glycoprotein. *Proc. Natl. Acad. Sci. USA* **82**, 2330–2333.
- Robinson, D.R., Kalyana-Sundaram, S., Wu, Y.M., Shankar, S., Cao, X., Ateeq, B., Asangani, I.A., Iyer, M., Maher, C.A., Grasso, C.S., et al. (2011). Functionally recurrent rearrangements of the MAST kinase and Notch gene families in breast cancer. *Nat. Med.* **17**, 1646–1651.
- Shabbir, M., and Stuart, R. (2010). Lestaurtinib, a multitargeted tyrosine kinase inhibitor: from bench to bedside. *Expert Opin. Investig. Drugs* **19**, 427–436.
- Siddik, Z.H. (2003). Cisplatin: mode of cytotoxic action and molecular basis of resistance. *Oncogene* **22**, 7265–7279.
- Valiente, M., Andres-Pons, A., Gomar, B., Torres, J., Gil, A., Tapparel, C., Antonarakis, S.E., and Pulido, R. (2005). Binding of PTEN to specific PDZ domains contributes to PTEN protein stability and phosphorylation by microtubule-associated serine/threonine kinases. *J. Biol. Chem.* **280**, 28936–28943.
- Verlhac, M.H., Lefebvre, C., Kubiak, J.Z., Umbhauer, M., Rassinier, P., Colledge, W., and Maro, B. (2000). Mos activates MAP kinase in mouse oocytes through two opposite pathways. *EMBO J.* **19**, 6065–6074.
- Wang, J., and Wu, G.S. (2014). Role of autophagy in cisplatin resistance in ovarian cancer cells. *J. Biol. Chem.* **289**, 17163–17173.
- Yamamoto, T., Tsigelny, I.F., Gotz, A.W., and Howell, S.B. (2015). Cisplatin inhibits MEK1/2. *Oncotarget* **6**, 23510–23522.

STAR★METHODS

KEY RESOURCES TABLE

REAGENT or RESOURCE	SOURCE	IDENTIFIER
Antibodies		
Mouse monoclonal anti-beta-actin (clone AC-15) antibody	Sigma-Aldrich	Cat#A1978; RRID: AB_476692
Mouse monoclonal anti-MBP (clone F-6) antibody	Santa Cruz Biotechnology	Cat#sc-271524; RRID: AB_10655672
Mouse monoclonal anti-glutathione S-transferase (clone GST-2) antibody	Sigma-Aldrich	Cat#G1160; RRID: AB_259845
Mouse monoclonal anti-myc (clone 9B11) antibody	Cell Signaling Technology	Cat#2276; RRID: AB_331783
Rabbit monoclonal anti-phospho-MEK S217/S221 (clone 41G9) antibody	Cell Signaling Technology	Cat#9154; RRID: AB_2138017
Rabbit polyclonal anti-phospho-MEK S221 (clone 166F8) antibody	Cell Signaling Technology	Cat#2338; RRID: AB_490903
Mouse monoclonal anti-MEK1 (clone 61B12) antibody	Cell Signaling Technology	Cat#2352; RRID: AB_10693788
Rabbit monoclonal anti-phospho-c-Raf (S338) (clone 56A6) antibody	Cell Signaling Technology	Cat#9427; RRID: AB_10078092
Rabbit polyclonal anti-c-Raf antibody	Cell Signaling Technology	Cat#9422; RRID: AB_390808
Mouse monoclonal anti-c-Raf (clone 53) antibody for immunoprecipitation	BD Biosciences	Cat#610152; RRID: AB_397553
Rabbit polyclonal phospho-p44/42 MAPK (Erk1/2) (T202/Y204) (clone 20G11) antibody	Cell Signaling Technology	Cat#4376; RRID: AB_331772
Rabbit monoclonal anti-p44/42 MAPK (Erk1/2) (clone 137F5) antibody	Cell Signaling Technology	Cat#4695; RRID: AB_390779
Mouse monoclonal anti-p44/42 MAPK (Erk1/2) (clone 3A7) antibody	Cell Signaling Technology	Cat#9107; RRID: AB_2235073
Rabbit monoclonal anti-BIM (clone C34C5) antibody	Cell Signaling Technology	Cat#2933; RRID: AB_1030947
Rabbit monoclonal anti-cleaved PARP (Asp214) (clone D64E10) XP antibody	Cell Signaling Technology	Cat#5625; RRID: AB_10699459
Rabbit polyclonal anti-Bcl-2 antibody	Cell Signaling Technology	Cat#2872; RRID: AB_10693462
Mouse monoclonal anti-BID (clone 5C9) antibody	Santa Cruz Biotechnology	Cat#sc-56025; RRID: AB_781628
Mouse monoclonal anti-Mcl-1 (clone 22) antibody	Santa Cruz Biotechnology	Cat#sc-12756; RRID: AB_627915
Mouse monoclonal anti-Bcl-xL (clone H-5) antibody	Santa Cruz Biotechnology	Cat#sc-8392; RRID: AB_626739
Rabbit monoclonal anti-phospho-BAD (S112) (clone 40A9) antibody	Cell Signaling Technology	Cat#5284; RRID: AB_560884
Rabbit monoclonal anti-BAD (clone D24A9) antibody	Cell Signaling Technology	Cat#9239; RRID: AB_2062127
Rabbit monoclonal anti-phospho-Histone gamma H2AX (S139) (clone 20E3) antibody	Cell Signaling Technology	Cat#9718; RRID: AB_2118009
Rabbit polyclonal anti-phospho-53BP1 (S1778) antibody	Cell Signaling Technology	Cat#2675; RRID: AB_490917
Rabbit monoclonal anti-Cisplatin-modified DNA (clone CP9/19) antibody	Abcam	Cat#ab103261; RRID: AB_10715243
Mouse monoclonal anti-FLAG (clone M2) antibody	Sigma-Aldrich	Cat#F1804; RRID: AB_262044
Rabbit polyclonal anti-FLAG antibody	Sigma-Aldrich	Cat#F7425; RRID: AB_439687
Mouse monoclonal anti-phospho-STAT3 (Y705) (clone B-7) antibody	Santa Cruz Biotechnology	Cat#sc-8059; RRID: AB_628292
Rabbit polyclonal anti-STAT3 (C-20) antibody	Santa Cruz Biotechnology	Cat#sc-482; RRID: AB_632440
Rabbit monoclonal anti-phospho-AKT (S473) (clone D9E) antibody	Cell Signaling Technology	Cat#4060; RRID: AB_2315049
Mouse monoclonal anti-AKT (clone 2H10) antibody	Cell Signaling Technology	Cat#2967; RRID: AB_331160
Rabbit polyclonal FANCD2 antibody	Novus Biologicals	Cat#NB100-182; RRID: AB_10002867
Rabbit polyclonal anti-phospho-ATR (S1989) antibody	GeneTex	Cat#GTX128145; RRID: AB_2687562

(Continued on next page)

Continued

REAGENT or RESOURCE	SOURCE	IDENTIFIER
Rabbit polyclonal anti-ATR antibody	Cell Signaling Technology	Cat#2790; RRID: AB_2227860
Rabbit monoclonal phospho-ATM (S1981) (clone EP1890Y) antibody	Abcam	Cat#ab81292; RRID: AB_1640207
Rabbit monoclonal anti-ATM (clone D2E2) antibody	Cell Signaling Technology	Cat#2873; RRID: AB_2062659
Rabbit monoclonal anti-phospho-Chk1 (S345) (clone 133D3) antibody	Cell Signaling Technology	Cat#2348; RRID: AB_331212
Mouse monoclonal anti-Chk1 (clone 2G1D5) antibody	Cell Signaling Technology	Cat#2360; RRID: AB_2080320
Rabbit polyclonal anti-phospho-Chk2 (T68) antibody	Cell Signaling Technology	Cat#2661; RRID: AB_331479
Rabbit polyclonal anti-Chk2 antibody	Cell Signaling Technology	Cat#2662; RRID: AB_2080793
Rabbit polyclonal anti-FANCE antibody	Bethyl	Cat#A302-125A; RRID: AB_1720357
Rabbit polyclonal anti-FANCG antibody	Novus Biologicals	Cat#NB100-2566; RRID: AB_921259
Rabbit polyclonal anti-FANCI antibody	Abcam	Cat#ab15344; RRID: AB_443182
Rabbit polyclonal anti-FANCA antibody	Bethyl	Cat#A301-980A; RRID: AB_1547945
Mouse monoclonal anti-FANCF (clone D-2) antibody	Santa Cruz Biotechnology	Cat#sc-271952; RRID: AB_10708556
Mouse monoclonal anti-FANCL (clone C-4) antibody	Santa Cruz Biotechnology	Cat#sc-137076; RRID: AB_2262590
Rabbit polyclonal anti-FAMCM antibody	Bethyl	Cat#A302-637A; RRID: AB_10567252
Mouse monoclonal anti-Histone H3 (clone 96C10) antibody	Cell Signaling Technology	Cat#3638; RRID: AB_1642229
Rabbit monoclonal anti-pan-Trk (clone A7H6R) antibody	Cell Signaling Technology	Cat#92991; RRID: N/A
Rabbit polyclonal anti-Fit-3/Flk-2 (C-20) antibody	Santa Cruz Biotechnology	Cat#sc-479; RRID: AB_631052
Rabbit monoclonal anti-Jak2 (clone D2E12) antibody	Cell Signaling Technology	Cat#3230; RRID: AB_2128522
Rabbit polyclonal anti-phospho BRaf (S445) antibody	Cell Signaling Technology	Cat#2696; RRID: AB_390721
Rabbit monoclonal anti-BRaf (clone 13) antibody	BD Biosciences	Cat#612374; RRID: AB_399736
Rabbit polyclonal anti-MAST1 antibody	Novus Biological	Cat#NBP2-17228; RRID: N/A
Rabbit polyclonal anti-MAST1 antibody for IHC	Novus Biological	Cat#NBP1-81453; RRID: AB_11061334
Rabbit monoclonal anti-Ki67 (clone EPR3610) antibody for IHC	Abcam	Cat#ab92742; RRID: AB_10562976
Rabbit polyclonal anti-phospho MEK (S218/S222) antibody for IHC	Abcam	Cat#ab194754; RRID: N/A
Biological Samples		
Human head and neck tumor tissues	This paper	N/A
Ovarian cancer patient-derived xenografts (PDX)	The Jackson Laboratory	Cat#TM000335
Head and neck cancer patient-derived xenografts (PDX)	This paper	N/A
Lung cancer patient-derived xenografts (PDX)	Owonikoko et al., 2016	N/A
Chemicals, Peptides, and Recombinant Proteins		
Cisplatin	Sigma-Aldrich	Cat#P4394; CAS: 15663-27-1
Carboplatin	Sigma-Aldrich	Cat#C2538; CAS: 41575-94-4
FlexiTube GeneSolution GS5894 for Raf1	Qiagen	Cat#1027416
Negative Control siRNA	Qiagen	Cat#1027310
Recombinant inactive MEK1	SignalChem	Cat#M02-14BG
Recombinant active MEK1	Thermo Fisher	Cat#PV3303
Recombinant active MEK1 for MST	Proqinase	Cat#0550-0000-3
Recombinant active c-Raf	SignalChem	Cat#R01-13G
Recombinant inactive ERK2	SignalChem	Cat#M28-14G
Myelic Basic Protein	Sigma-Aldrich	Cat#M1891
Mitomycin C	Sigma-Aldrich	Cat#M4287; CAS: 50-07-7
Camptothecin	Selleckchem	Cat#S1288; CAS: 7689-03-4
Doxorubicin	Sigma-Aldrich	Cat#D1515; CAS: 13192-04-6
Paclitaxel	MilliporeSigma	Cat#580555; CAS: 25316-40-9
Lestaurtinib	LC Laboratories	Cat#L-6307; CAS: 111358-88-4

(Continued on next page)

Continued

REAGENT or RESOURCE	SOURCE	IDENTIFIER
Dovitinib	LC Laboratories	Cat#D-3608; CAS: 405169-16-6
Staurosporine	Sigma-Aldrich	Cat#M1323; CAS: 62996-74-1
Midostaurin	LC Laboratories	Cat#P-7600; CAS: 120685-11-2
Sunitinib	LC Laboratories	Cat#S-8877; CAS: 557795-19-4
SU14813	MedKoo	Cat#; CAS: 627908-92-3
Bosutinib	LC Laboratories	Cat#B-1788; CAS: 380843-75-4
Ruxolitinib	LC Laboratories	Cat#R-6600; CAS: 941678-49-5
SB203580	LC Laboratories	Cat#S-3400; CAS: 152121-47-6
Ruboxistaurin	Sigma-Aldrich	Cat#SML0693; CAS: 169939-93-9
MLN518	Selleckchem	Cat#S1043; CAS: 387867-13-2
AC220	Selleckchem	Cat#S1526; CAS: 950769-58-1
GNF5837	Selleckchem	Cat#S7519; CAS: 1033769-28-6
GW441756	Selleckchem	Cat#S2891; CAS: 504433-23-2
Fedratinib	Selleckchem	Cat#S2736; CAS: 936091-26-8
AZD1480	Selleckchem	Cat#S2162; CAS: 935666-88-9
AZD6244	Selleckchem	Cat#S1008; CAS: 606143-52-6
Trametinib	Selleckchem	Cat#S2673; CAS: 871700-17-3
Critical Commercial Assays		
FITC Annexin V Apoptosis Detection Kit	BD Biosciences	Cat#556547
CellTiter-Glo Luminescent Viability Assay	Promega	Cat#G7570
ADP-Glo Kinase Assay	Promega	Cat#V6930
Chromatin Extraction Kit	Abcam	Cat#ab117152
Phospho Explorer Antibody Array	Full Moon Biosystems	Cat#PEX100
Ras Activation ELISA Assay Kit	EMD Millipore	Cat#17-497
Amine Coupling Kit	GE Healthcare Life Sciences	Cat#BR100050
Sensor Chip CM5	GE Healthcare Life Sciences	Cat#BR100399
Protein Thermal Shift Dye Kit	ThermoFisher	Cat#4461146
High-Capacity cDNA Reverse Transcription Kit	Applied Biosystems	Cat#4368814
Experimental Models: Cell Lines		
Human: A549 cells	ATCC	Cat#CCL-185
Human: A549 cisplatin resistant cells	This paper	N/A
Human: HCC827 cells	ATCC	Cat#CRL-2868
Human: H358 cells	ATCC	Cat#CRL-5807
Human: H1299 cells	ATCC	Cat#CRL-5803
Human: H460 cells	ATCC	Cat#HTB-177
Human: H1975 cells	ATCC	Cat#CRL-5908
Human: Calu-1 cells	ATCC	Cat#CRL-5807
Human: H157 cells	ATCC	Cat#CRL-5802
Human: H128 cells	ATCC	Cat#HTB-120
Human: H146 cells	ATCC	Cat#HTB-173
Human: H187 cells	ATCC	Cat#CRL-5804
Human: H209 cells	ATCC	Cat#HTB-172
Human: H526 cells	ATCC	Cat#CRL-5811
Human: DMS53 cells	ATCC	Cat#CRL-2062
Human: DMS114 cells	ATCC	Cat#CRL-2066
Human: DMS153 cells	ATCC	Cat#CRL-2064
Human: SW-626 cells	ATCC	Cat#HTB-78
Human: SK-OV-3 cells	ATCC	Cat#HTB-77
Human: OVCAR-3 cells	ATCC	Cat#HTB-161

(Continued on next page)

Continued

REAGENT or RESOURCE	SOURCE	IDENTIFIER
Human: Caov-3 cells	ATCC	Cat#HTB-75
Human: BG-1 cells	Geisinger et al., 1989	RRID: CVCL_6570
Human: 1A9 cells	Geisinger et al., 1989	RRID: CVCL_H619
Human: MDA686TU cells	Lin et al., 2007	RRID: CVCL_6985
Human: Tu-212 cells	Lin et al., 2007	RRID: CVCL_4915
Human: PCI-37B cells	Lin et al., 2007	RRID: CVCL_C759
Human: UM-SCC-1 cells	Lin et al., 2007	RRID: CVCL_7707
Human: PCI-15A cells	Lin et al., 2007	RRID: CVCL_C184
Human: PCI-15A cisplatin resistant cells	This paper	N/A
Human: 212LN cells	Lin et al., 2007	RRID: CVCL_1T18
Human: UDSCC2 cells	Lin et al., 2007	RRID: CVCL_E325
Human: UM-SCC-47 cells	Lin et al., 2007	RRID: CVCL_7759
Human: 93-VU-147T cells	Lin et al., 2007	COSS2296308
Human: Tu-167 cells	Lin et al., 2007	RRID: CVCL_4912
Human: FaDu cells	Lin et al., 2007	RRID: CVCL_1218
Human: UM-SCC-22B cells	Lin et al., 2007	RRID: CVCL_7732
Human: JHU022 cells	Lin et al., 2007	RRID: CVCL_5991
Human: 1483 cells	Lin et al., 2007	RRID: CVCL_6980
Human: PCI-13 cells	Lin et al., 2007	RRID: CVCL_C182
Human: SqCC/Y1 cells	Lin et al., 2007	RRID: CVCL_0551
Human: KB-3-1 cells	Richert et al., 1985	RRID: CVCL_2088
Human: KB-3-1 cisplatin resistant cells	Richert et al., 1985	RRID: CVCL_IP04
Human: A2780 cells	Sigma Aldrich	Cat#93112519
Human: A2780 cisplatin resistant cells	Sigma Aldrich	Cat#93112517
Human: MV-4-11 cells	ATCC	Cat#CRL-9591
Human: HEL cells	ATCC	Cat#TIB-180
Experimental Models: Organisms/Strains		
Mouse: Hsd:Athymic Nude-Foxn1nu	Envigo	Cat#069
Mouse: NOD.CB17-Prkdc ^{scid} /NCrCrI	Charles Rivers	Cat#394; RRID: IMSR_CRL:394
Mouse: NOD.Cg-Prkdc ^{scid} Il2rg ^{tm1Wjl} /SzJ	The Jackson Laboratory	Cat#JAX:005557; RRID: IMSR_JAX:005557
Oligonucleotides		
TRC Human Kinase shRNA Gene Family Library	Dharmacon	Cat#RHS4884
shRNA targeting sequence: MAST1 #1: CCACTT CCTCTCCAAACACTT	Dharmacon	Cat#RHS3979-9588955
shRNA targeting sequence: MAST1 #2: CCACG GTCTACTTCTATGAAT	Dharmacon	Cat#RHS3979-9588953
shRNA targeting sequence: MAST1 #3: CGTGAT GATGAATCACGTCTA	Dharmacon	Cat#RHS3979-9588952
shRNA targeting sequence: MEK1 #1: CTGATGC TGAGGAAGTGGATT	Dharmacon	Cat#RHS3979-9570884
shRNA targeting sequence: MEK1 #2: GATTACA TAGTCAACGAGCCT	Dharmacon	Cat#RHS3979-9570886
shRNA targeting sequence: JAK2 #1: CAGTGTTA GATATGATGAGAA	Dharmacon	Cat#RHS3979-9571807
shRNA targeting sequence: JAK2 #2: GCTTTGTC TTTCGTGCATTA	Dharmacon	Cat#RHS3979-9571810
Primer: MAST1 shRNA resistant silent-mutant Forward GTGGACGAGCTCCACTTCTATCAAAACACTTCGGG AGCACC	This paper	N/A

(Continued on next page)

Continued

REAGENT or RESOURCE	SOURCE	IDENTIFIER
Primer: MAST1 shRNA resistant silent-mutant Reverse GGTGCTCCCGAAGTGTGTTTGGATAGGAAGTGGAGCTC GTCCAC	This paper	N/A
Primer: MAST1 Forward TCTCTGGACCGCGCTTTCTA	This paper	N/A
Primer: MAST1 Reverse TGAGGCTTTTCCGATTACTGGT	This paper	N/A
Primer: FLT3 Forward GAATTCCCATGAAGCCCTGA	This paper	N/A
Primer: FLT3 Reverse CCCACTTTCCAATCACATCCA	This paper	N/A
Primer: JAK2 Forward TCTGGGGAGTATGTTGCAGAA	This paper	N/A
Primer: JAK2 Reverse AGACATGGTTGGTGGATACC	This paper	N/A
Primer: TrkA Forward AACCTCACCATCGTGAAGAGT	This paper	N/A
Primer: TrkA Reverse TGAAGGAGAGATTCAGGCGAC	This paper	N/A
Primer: GAPDH Forward GACATCAAGAAGGTGGTGAA	This paper	N/A
Primer: GAPDH Reverse TGTCCATACCAGGAAATGAGC	This paper	N/A
Recombinant DNA		
Plasmid: pLHCX	Clontech	Cat#S1866
Plasmid: Gateway pDEST27	Invitrogen	Cat#11812013
Plasmid: pLHCX-Gateway	This paper	N/A
Plasmid: pLHCX-myc-MAST1 WT	This paper	N/A
Plasmid: pLHCX-myc-MAST1 D497A	This paper	N/A
Plasmid: pDEST27-MAST1 WT	This paper	N/A
Plasmid: pDEST27-MAST1 D497A	This paper	N/A
Plasmid: pDEST27-MAST1 L504D	This paper	N/A
Plasmid: pLHCX-flag-MEK1 S221A	This paper	N/A
Plasmid: pLHCX-flag-MEK1 S221D	This paper	N/A
Software and Algorithms		
GraphPad Prism software	GraphPad Software	http://www.graphpad.com

CONTACT FOR REAGENT AND RESOURCE SHARING

Further information and requests for resources and reagents should be directed to and will be fulfilled by the Lead Contact, Sumin Kang (smkang@emory.edu).

EXPERIMENTAL MODEL AND SUBJECT DETAILS

Human Studies

Approval to use human specimens was given by the Institutional Review Board of Emory University. All clinical samples were collected with informed consent under Health Insurance Portability and Accountability Act (HIPAA) approved protocols.

Animal Studies

Animal experiments were performed according to protocols approved by the Institutional Animal Care and Use Committee of Emory University. Nude mice (athymic nu/nu, female, 4–6-week old, Envigo) or NSG mice (NOD scid gamma, female, 4–6-week old, Jackson Laboratory) were used for xenograft experiments.

Cell Culture

H128 cells were cultured in Iscove Modified Dulbecco Medium (IMDM) with 20% FBS. DMS53, DMS114, and DMS153 cells were cultured in Waymouth medium with 10% FBS. SK-OV-3 cells were cultured in McCoy's 5a medium with 10% FBS. SW-626 cells were cultured in Leibovitz's L15 medium with 10% FBS. All HNSCC cell lines were cultured in Dulbecco Modified Eagle Medium (DMEM)/Ham's F-12 50/50 mix medium with 10% FBS. KB-3-1, BG-1, Caov-3, and 293T cells were cultured in DMEM with 10% FBS. All the rest were cultured in RPMI 1640 medium with 10% FBS.

METHOD DETAILS

RNAi Screens

Primary screen was performed using the human kinome shRNA library by transducing KB-3-1 cisplatin-resistant human carcinoma cells (KB-3-1^{cisR}) with lentivirus pools targeting each gene individually. Cells were seeded into 6 replicates and infected with lentivirus in 96-well plates. 48 hr after infection, cells were treated with PBS, a sublethal dose of cisplatin, or puromycin (0.5 $\mu\text{g}/\text{ml}$), in duplicates. Cell viability was determined after 2 days of cisplatin treatment using CellTiter-Glo Luminescent Viability Assay (Promega). Gene candidates that induced more than 15% cell death by shRNA alone and/or had poor shRNA virus transduction efficacy assessed by puromycin selection were excluded. The 50 top ranking candidates from the primary screen were further confirmed in four cisplatin-resistant cancer cell lines PCI-15A^{cisR}, A549^{cisR}, A2780^{cisR}, and KB-3-1^{cisR} as performed in primary screen.

Virus Production and Infection for Protein Overexpression in Cancer Cells

Human MAST1 and MEK1 were myc or flag tagged by PCR and subcloned into pDEST27 and pLHCX-derived Gateway destination vectors. Selection was carried out with 300 $\mu\text{g}/\text{ml}$ hygromycin for stable expression. MAST1 and MEK1 variants were generated by site-directed mutagenesis. Lentivirus carrying shRNA were generated by transfecting 293T cells with pLKO.1 vector encoding shRNA, pMD2.G, and psPAX2 and virus were collected. Cells were infected with lentivirus for 2 days and selected using puromycin (2 $\mu\text{g}/\text{ml}$).

Cell Viability Assay, Colony Formation Assay, and Apoptosis Assay

Cells were treated with 5 $\mu\text{g}/\text{ml}$ cisplatin for 48 hr for Cis^R cells and 24 hr for parental cells unless specifically indicated. Approximately 7000 cells/well were seeded in 96-well plates and treated with the indicated concentrations of cisplatin and lestaurtinib for 48 hr. Cell viability was measured using CellTiter-Glo Luminescent Viability Assay according to the manufacturer's instructions. For colony forming assay, 200-500 cells were seeded in 35-mm dishes and treated with PBS, cisplatin, lestaurtinib or in combination for 24-48 hr. The colonies were stained with 0.5% crystal violet and counted by ImageJ software after 10 days. Apoptotic cells were assessed using FITC Annexin V Apoptosis Detection kit.

Kinase Activity Assays

MAST1 variants were precipitated from cell lysates with a glutathione-Sepharose 4B column or anti-MAST1 antibody. Eluted MAST1 was incubated with MBP or inactive MEK1 in kinase assay buffer (40 mM Tris-HCl [pH 7.5], 20 mM MgCl₂, 200 μM ATP, 0.1 mg/ml BSA) for 30 min at 30°C. The activity of MAST1 was determined either by ADP-Glo Kinase Assay or Western blot using phospho-MEK S217/S221 antibody. cRaf and MEK1 kinase activities were measured by ADP-Glo kinase assay using recombinant inactive MEK1 and ERK2 as substrates, respectively.

Cisplatin or Carboplatin Sensitivity Assay

To determine the IC₅₀ of patient-derived xenograft (PDX) tumors, PDX tumors were digested with tissue dissociation buffer (0.1% collagenase, 0.01% hyaluronidase, 0.01% DNase I in HBSS) for 1 hr at 37°C to obtain single cell suspension. The enzyme digestion-released tumor cells were washed through a 70 mm strainer with HBSS and counted. 1~2 $\times 10^4$ of live tumor cells for each PDX tumor were seeded in 96 well plates and treated with different concentrations of cisplatin or carboplatin. After 48~72 hr, the cell viability was determined by Cell Titer Glo assay and IC₅₀ was calculated using Graphpad software with non-linear regression analysis. For cancer cell lines, approximately 0.5~1 $\times 10^4$ of cells were seeded in 96 well plates and treated with different concentrations of cisplatin. After 48~72 hr, the cell viability was determined by Cell Titer Glo assay and IC₅₀ was calculated using Graphpad software.

Phospho-Protein Profiling

Lysates obtained from KB-3-1^{cisR}-pLKO.1 and KB-3-1^{cisR}-pLKO.1-MAST1 shRNA cells treated with PBS or cisplatin were applied to the Phospho Explorer Antibody Array (Full Moon Biosystems), as previously described (Kang et al., 2010).

Surface Plasmon Resonance (SPR)

Biacore X100 system (GE Healthcare) was used to perform SPR experiments. 1 μM of recombinant MEK1 or RAF1 were coupled to CM5 sensor chip through amine chemistry at pH 5. For cisplatin-MEK1 or cisplatin-RAF1 binding analysis, a series dilution of cisplatin was prepared in 0.01 M HEPES pH 7.4, 0.15 M NaCl, 0.005% v/v Surfactant P20 and injected over MEK1 or RAF1 at 30 $\mu\text{l}/\text{min}$ for a contact time of 180 s at 20°C. For analysis of MAST1-MEK1 or RAF1-MEK1 interaction, single-cycle kinetic analysis was performed. Recombinant GST-MAST1 (0-100 nM) or GST-RAF1 (0-250 nM) at a series dilution were injected over the MEK1-coupled sensor chip in the absence or presence of 1 μM of cisplatin. The raw sensorgrams were blank-subtracted and analyzed using BIAevaluation Software (GE Healthcare).

Thermal Shift Assay

Thermal shift assay (Differential scanning fluorimetry) was performed using the Protein Thermal Shift Dye Kit. 1 μM of recombinant MEK1 or RAF1 was incubated with different concentrations of cisplatin. The fluorescence was recorded using Real-Time PCR

Systems (Applied Biosystems) and data were analyzed using Prism Graphpad with Boltzmann model. The dissociation constant (K_d) was calculated using the equation below:

$$Y = \text{Bottom} + \frac{(\text{Top} - \text{Bottom}) * (1 - ((P - K_d - X + \sqrt{((P + X + K_d)^2 - (4 * P * X)) / (2 * P))})}{2 * P}$$

MicroScale Thermophoresis (MST)

A serial dilution of cisplatin was prepared (61 nM ~ 2 mM) in assay buffer (14 mM HEPES pH 7.5, 105 mM NaCl, 3.5 mM MgCl₂, 0.04% Tween-20). 5 μ l of each dilution step were mixed with 5 μ l of the fluorescence-labeled recombinant MEK1 and filled in capillaries. The samples were analyzed on Monolith NT.115 Pico at 25°C, with 10% LED power and 80% Laser power. No sample aggregation or precipitation effects were observed in the normalized fluorescence.

Immunohistochemical Staining

Formalin-fixed, paraffin-embedded tissue specimens from HNSCC patients were obtained from the Emory head and neck tissue bank. Approval to use human specimens was given by the Institutional Review Board (IRB) of Emory University. Clinical information for the patients was obtained from the pathology files at Emory University Hospital under the guidelines and with approval from the IRB of Emory University. All clinical samples were collected with informed consent under Health Insurance Portability and Accountability Act approved protocols. Tumors from HNSCC patients who received platinum or non-platinum-based therapy were used. IHC analyses of MAST1, phospho-MEK S217/S221, and Ki-67 were performed according to the protocol described previously (Li et al., 2013). Positive staining of MAST1 and phospho-MEK1 in the tumor cells was identified using IHC signal intensity, scored as 0 to 3+.

Xenograft Studies

Animal experiments were performed according to protocols approved by the Institutional Animal Care and Use Committee of Emory University. Athymic nude mice (athymic nu/nu, 6-week old, Envigo) were subcutaneously injected with 5×10^5 KB-3-1^{cisR} cells with MAST1 knockdown and MEK1 variant expression. Cisplatin 5 mg/kg twice a week and lestaurtinib 20 mg/kg 5 times a week were administered by intraperitoneal (i.p.) injection and subcutaneous injection, respectively, from 3-7 days after xenograft for 16-28 days. For PDX mouse model, after informed consent and approval by the IRB of Emory, tumor tissues from a HNSCC patient and SCLC patients were biopsied and implanted into the hind flanks of 6-week old NOD scid mice (Charles River). Once the tumor size reached 1500 mm³, the tumor was excised and small pieces were implanted in the flank of 6-week old athymic nude mice. Ovarian cancer PDX donor mouse was obtained from Jackson Labs and serially transplanted to 6-week-old NOD scid gamma (NSG) mice. The mice were evenly divided into groups when the size of the tumor reached 100-150 mm³. Lestaurtinib was administered by subcutaneous injection of 20 or 30 mg/kg 5 times a week for 20-30 days. 40% polyethylene glycol 400, 10% povidone, and 2% benzyl alcohol in PBS was a diluent control. The combination group was given both cisplatin and lestaurtinib as described. Tumor growth was recorded by blind measurement of two perpendicular diameters of the tumors and tumor size was calculated using the formula $4\pi/3 \times (\text{width}/2)^2 \times (\text{length}/2)$. Tumors were harvested at the experimental endpoint and tumor proliferation was determined by Ki-67 IHC staining. For all animal studies, animals were randomly chosen. Concealed allocation and blinding of outcome assessment were used. No statistical method was used to predetermine sample size.

Cellular Thermal Shift Assay

Cellular thermal shift assay was performed as previously described (Gad et al., 2014; Martinez Molina et al., 2013). In brief, KB-3-1 cells with MAST1 knockdown were transfected with shRNA-resistant GST-fused MAST1 WT or L504D, and treated with DMSO or lestaurtinib (100 nM) for 24 hr. Cells were collected and resuspended in TBS. Multiple aliquots of cells were heated at 48, 50, 52, 54, 56, 58, 60, 62 and 64°C for 3 min. Cells were lysed, precipitates were removed, and the MAST1 in the soluble fraction was quantified by Western blot analyses.

QUANTIFICATION AND STATISTICAL ANALYSIS

Statistical analysis and graphical presentation was performed using Prism 6.0 (GraphPad). No statistical method was used to predetermine sample size. Data shown are from one representative experiment of multiple experiments. Data with error bars represent mean \pm standard deviation (SD), except for xenograft tumor growth curves, which represent mean \pm standard error of the mean (SEM). Statistical analysis of significance was based on paired two-tailed Student's *t* test for Figure 6D and non-paired for all other figures. Statistical tests performed are based on a set of assumptions including normal distribution and homogeneity of variances. The variability within each group has been quantified with standard deviation and used for statistical comparison.

DATA AND SOFTWARE AVAILABILITY

GraphPad Prism 6 was used in this study for graphics and statistical analyses.